

# Waves and fluctuations associated with local instabilities in the solar wind

---

Stuart D. Bale

Physics Department and Space Sciences Laboratory  
University of California, Berkeley

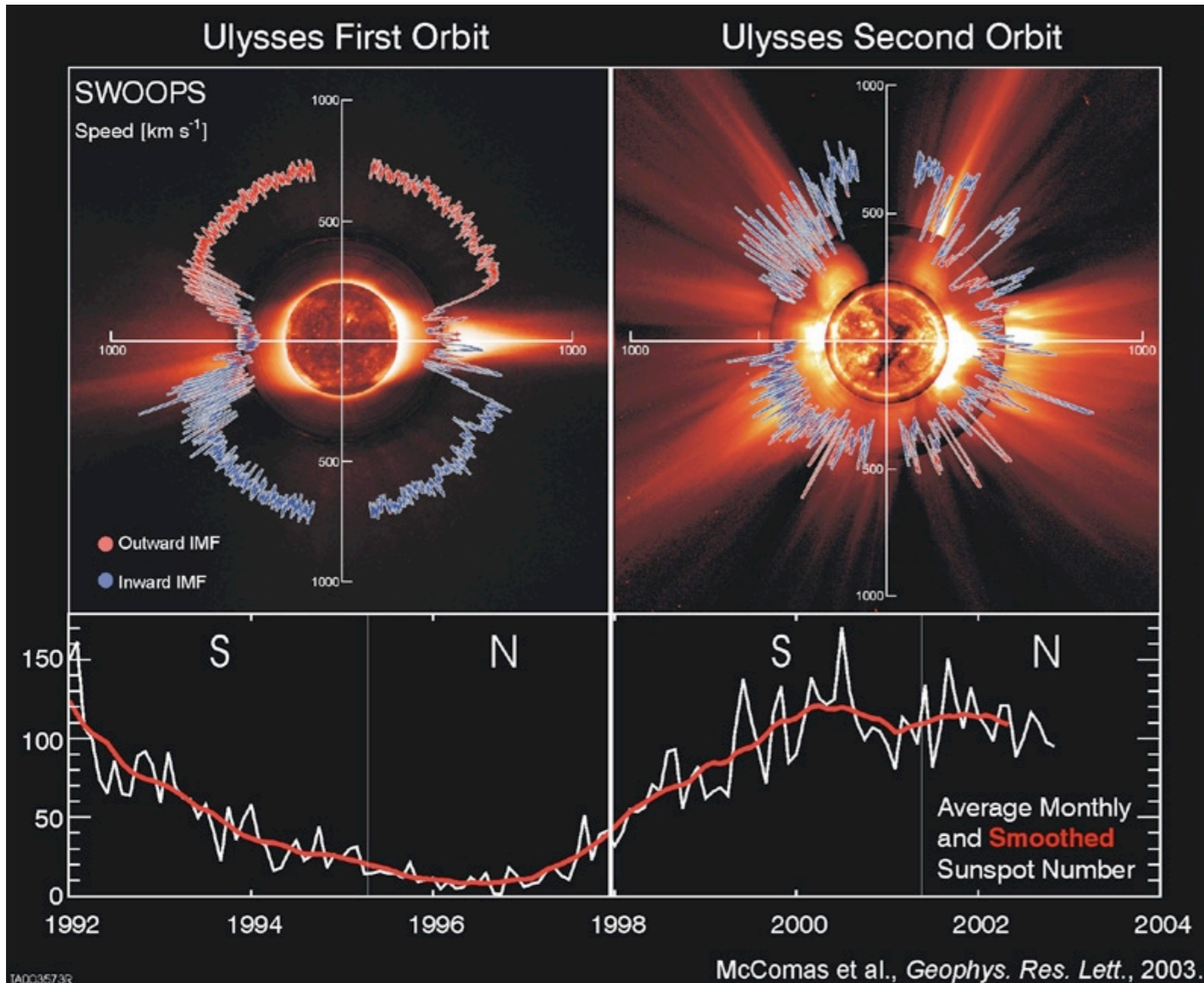
# plan

---

- Solar wind properties and turbulence
- Plasma physics measurements in the solar wind
- Instabilities (as opposed to ‘turbulence’)
- For the future...

Thesis: there is finite power at and above  $k\rho \sim 1$  that is unrelated to the turbulent cascade

# Solar wind properties (at, say, 1 AU)



## Fast wind (1 AU)

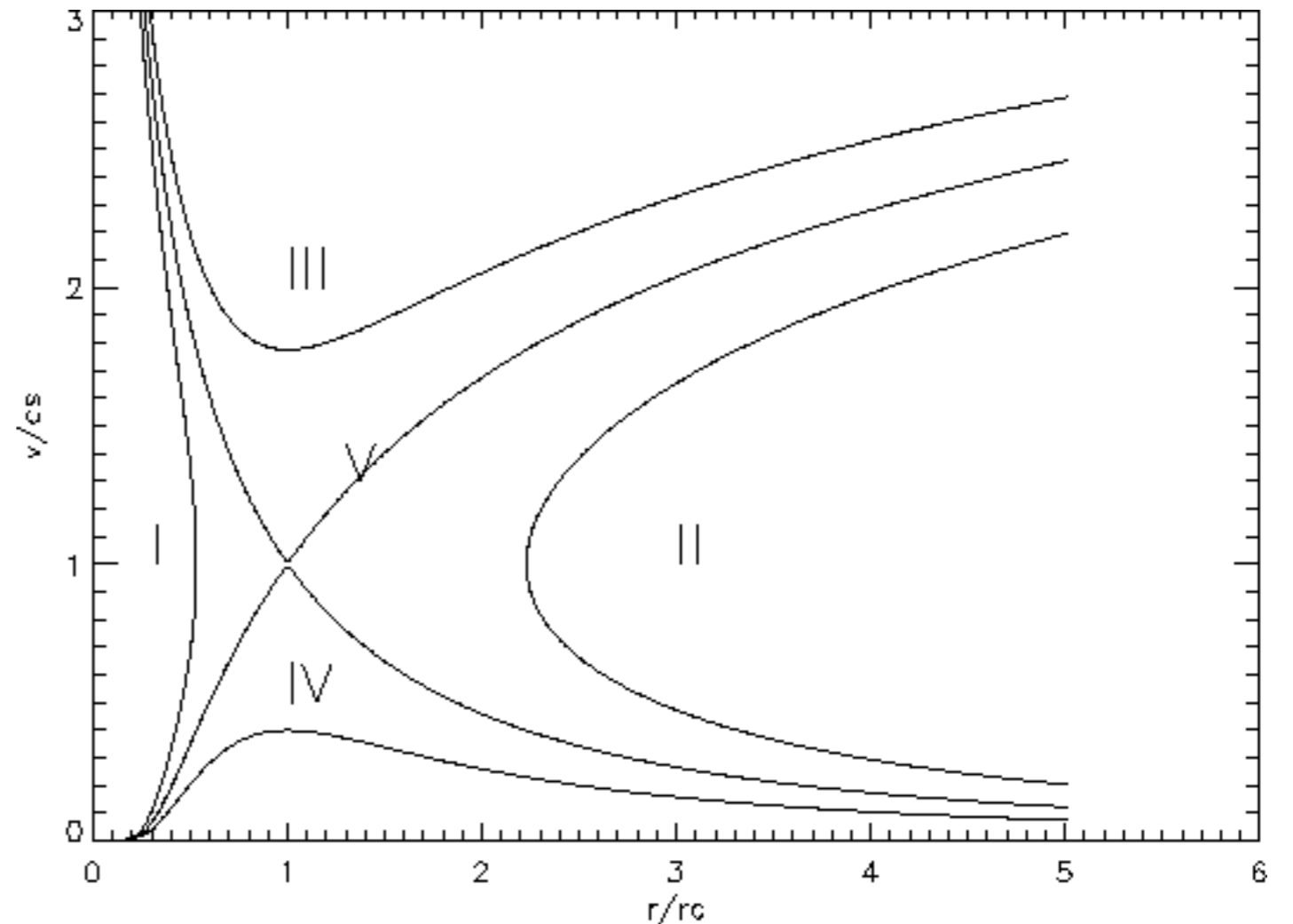
$v_{\text{sw}} \sim 500\text{-}1000 \text{ km/s}$   
 $T_p \sim 10\text{-}20 \text{ eV}$   
 $T_e \sim 5\text{-}20 \text{ eV}$   
 $n \sim 1\text{-}10 \text{ cm}^{-3}$   
 $B \sim 5 \text{ nT}$ ,  $\delta B$  is larger  
 $\beta \sim 1$

## Slow wind (1 AU)

$v_{\text{sw}} \sim 250\text{-}500 \text{ km/s}$   
 $T_p \sim 5\text{-}20 \text{ eV}$   
 $T_e \sim 5\text{-}20 \text{ eV}$   
 $n \sim 5\text{-}25 \text{ cm}^{-3}$   
 $B \sim 5 \text{ nT}$   
 $\beta \sim 1$

# 'Heating' is required to accelerate the solar wind

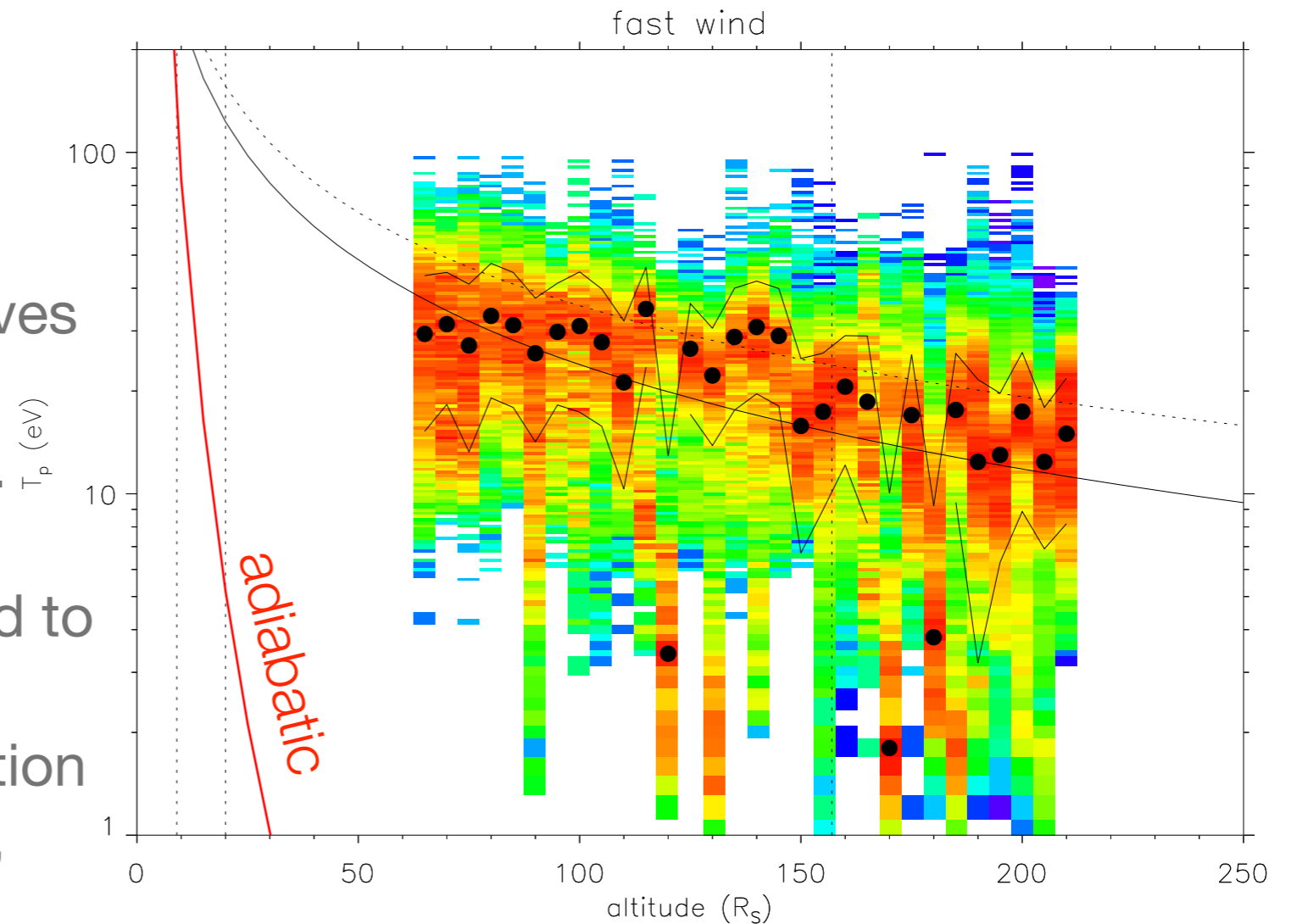
- Parker solar wind model (unmagnetized, zero angular momentum, critical points, etc.)
- Requires energy input at exobase *beyond* available photospheric thermal energy
- Plenty of magnetic energy density available
  - waves
  - reconnection
  - ambipolar electric field (exosphere)



(Parker, 1958)

# 'Heating' is required to sustain the solar wind

- Local ( $R_s$ ) and extended (AU) heating are required
- Extended heating implies waves
- Alfvén waves -
  - observed and copious (i.e. Belcher & Davis, 1971)
  - weakly damped (compared to fast- and slow-mode)
  - excited by large-scale motion near the Sun, n-i coupling, etc.



Helios proton temperature in the fast wind

Hence, turbulence...

# Alfvenic turbulence and heating

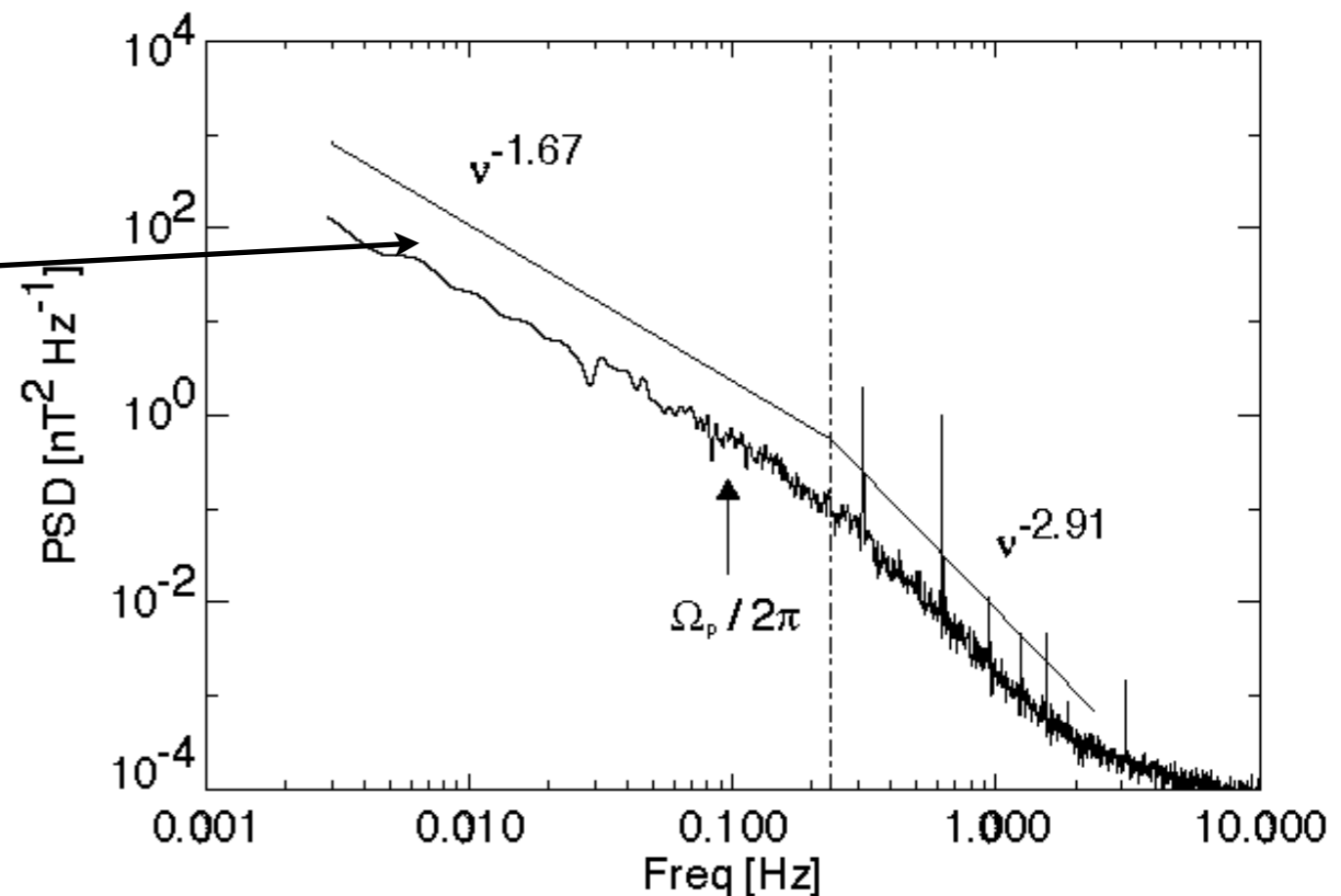
- Kolmogorov (isotropic, hydro) turbulence - scale free inertial range

$$\epsilon \sim \frac{u^2}{\tau} = \text{const} \quad \tau \sim \lambda/u$$

$$\epsilon \sim u^3/\lambda \quad u \sim (\epsilon\lambda)^{1/3}$$

$$P \sim \lambda u^2 \sim \epsilon^{2/3} \lambda^{5/3}$$

The total field  $|B|$ , field components, density, temperature, and velocity *all* show evidence of  $k^{-5/3}$  behavior (sometimes)



(Leamon et al., 1998)

# Alfvenic turbulence and heating

---

- Goldreich-Sridhar (anisotropic) turbulence - also scale free, 'strong'

perpendicular cascade  $k_{\parallel} \ll k_{\perp}$

critical balance  $\omega \sim k_{\parallel} v_A \sim k_{\perp} v_{\perp}$

$$\epsilon \sim \frac{v_{\perp}^2}{\tau} = \text{const}$$

$$\tau \sim \lambda / v_{\perp} \sim l_{\parallel} / v_A$$

$$\epsilon \sim v_{\perp}^3 / \lambda$$

$$v_{\perp} \sim (\epsilon \lambda)^{1/3}$$

$$P \sim \lambda u_{\perp}^2 \sim \epsilon^{2/3} \lambda^{5/3}$$

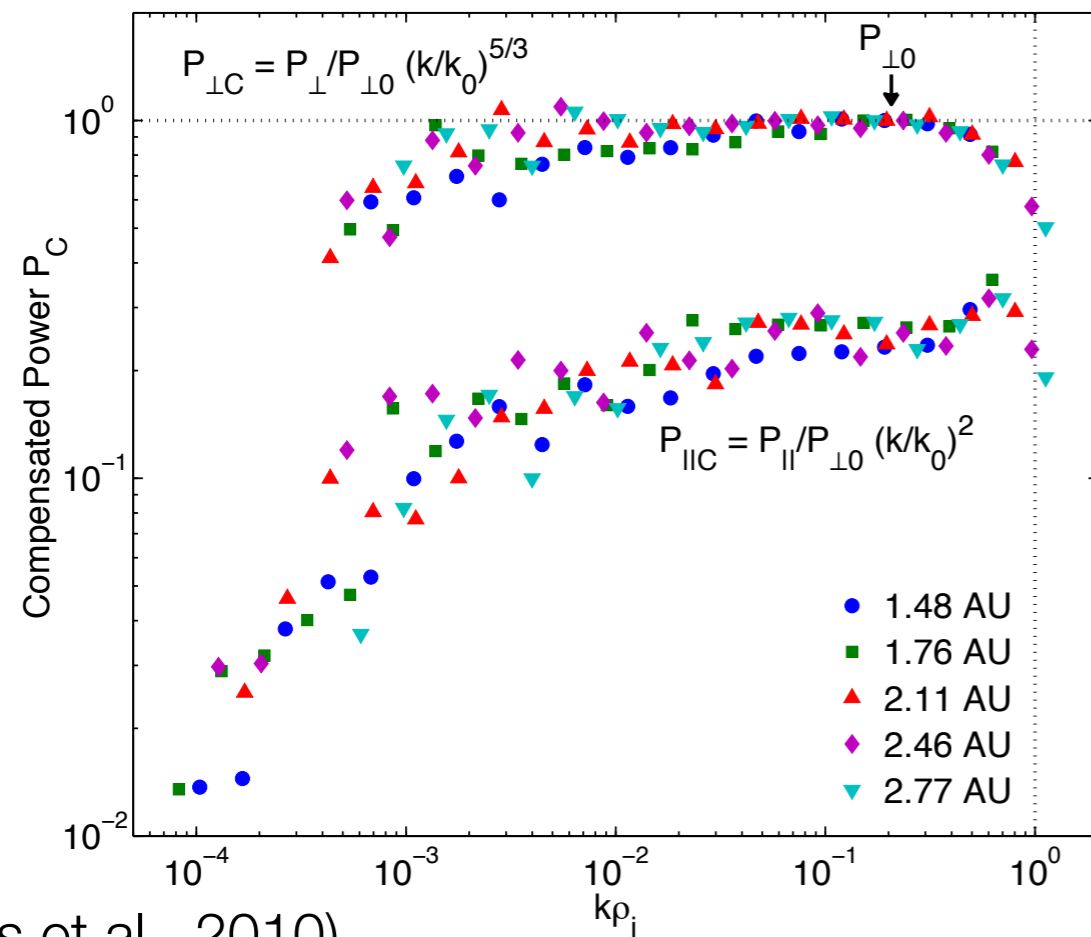
$$P_{\parallel} \sim l^2$$

$$k_{\parallel} \sim k_{\perp}^{2/3}$$

evolution is primarily in perpendicular wavenumber

# Evidence for a perpendicular cascade

- Magnetic field fluctuation power shows  $k^{-5/3}$  spectrum in the perp direction only
- Parallel power  $\ll$  perpendicular power
- Indices at high frequencies consistent with evolution to KAW



(Wicks et al., 2010)

**Figure 4.** Perpendicular and parallel power for each of the five periods in Table 1, compensated to remove a spectral gradient of  $-5/3$  from the perpendicular power and  $-2$  from the parallel.

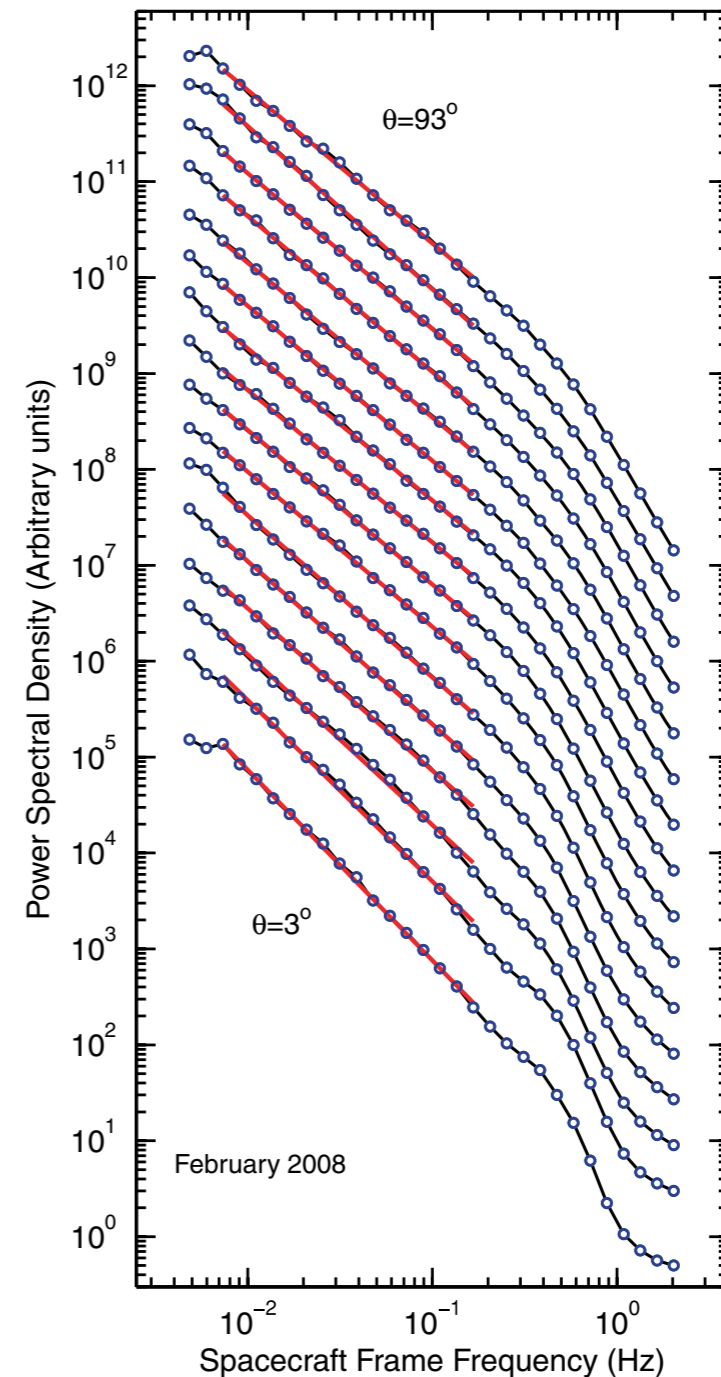


**Figure 5.** Power spectral density vs. frequency for angle bins centered at  $\theta = 3$  (bottom), 9, 15, 21, ..., 93 deg (top) computed using the 2008 February data in Table 1 by means of Equation (27). The different curves have been offset vertically for easier viewing.

(A color version of this figure is available in the online journal.) (Podesta, 2009)



# Alfvenic turbulence and heating

- Goldreich-Sridhar (anisotropic) turbulence - also scale free

perpendicular cascade  $k_{\parallel} \ll k_{\perp}$

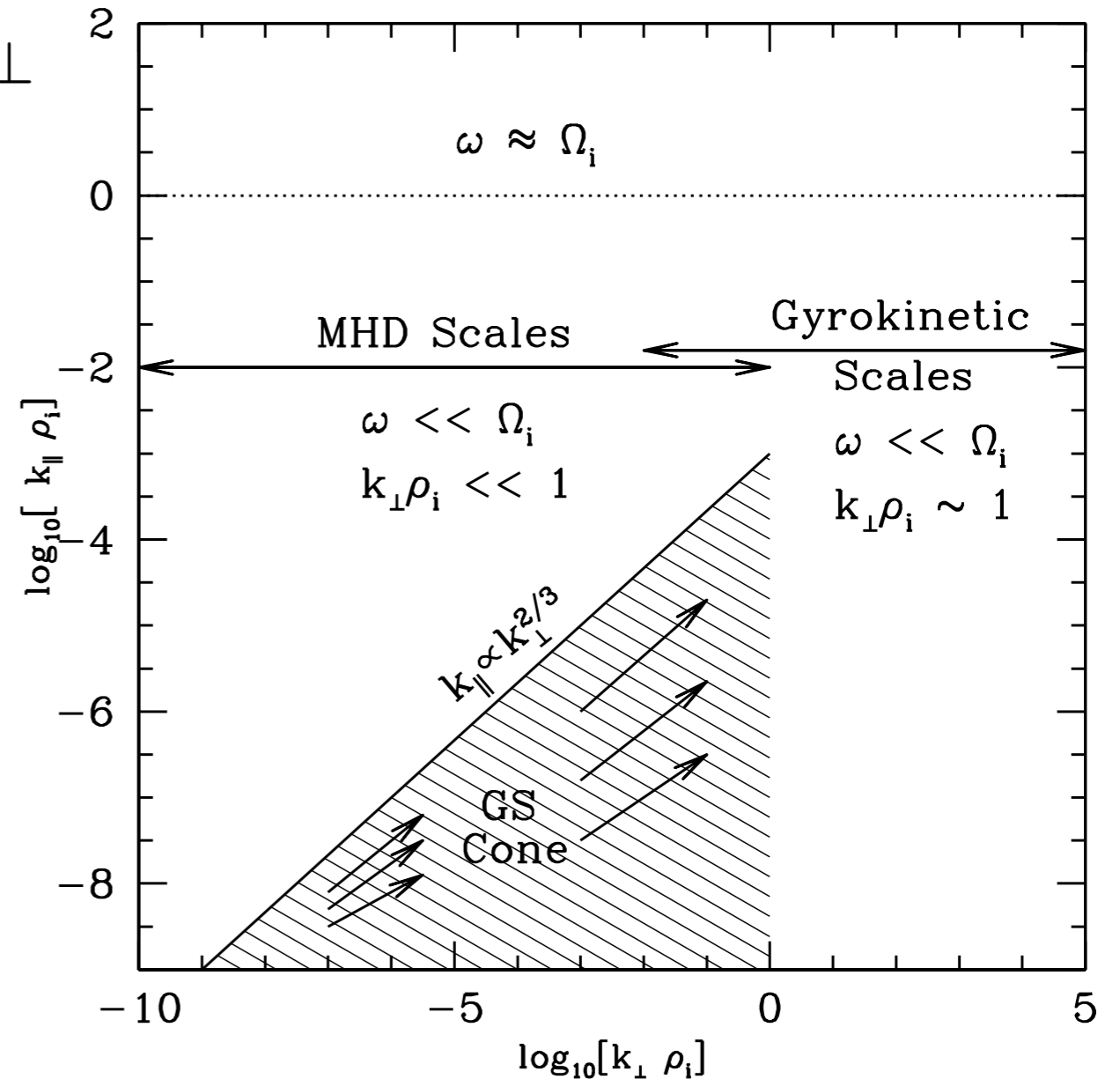
critical balance  $\omega \sim k_{\parallel} v_A \sim k_{\perp} v_{\perp}$

At  $k_{\perp} \rho_i \approx 1$

$$\omega / \Omega_i \approx (\rho_i / L)^{1/3} \beta_i^{-1/2}$$

is very small. Far from cyclotron resonance! So we think that  $\omega = k v_{sw}$  is pretty good.

Heating is by Landau damping or transit-time damping

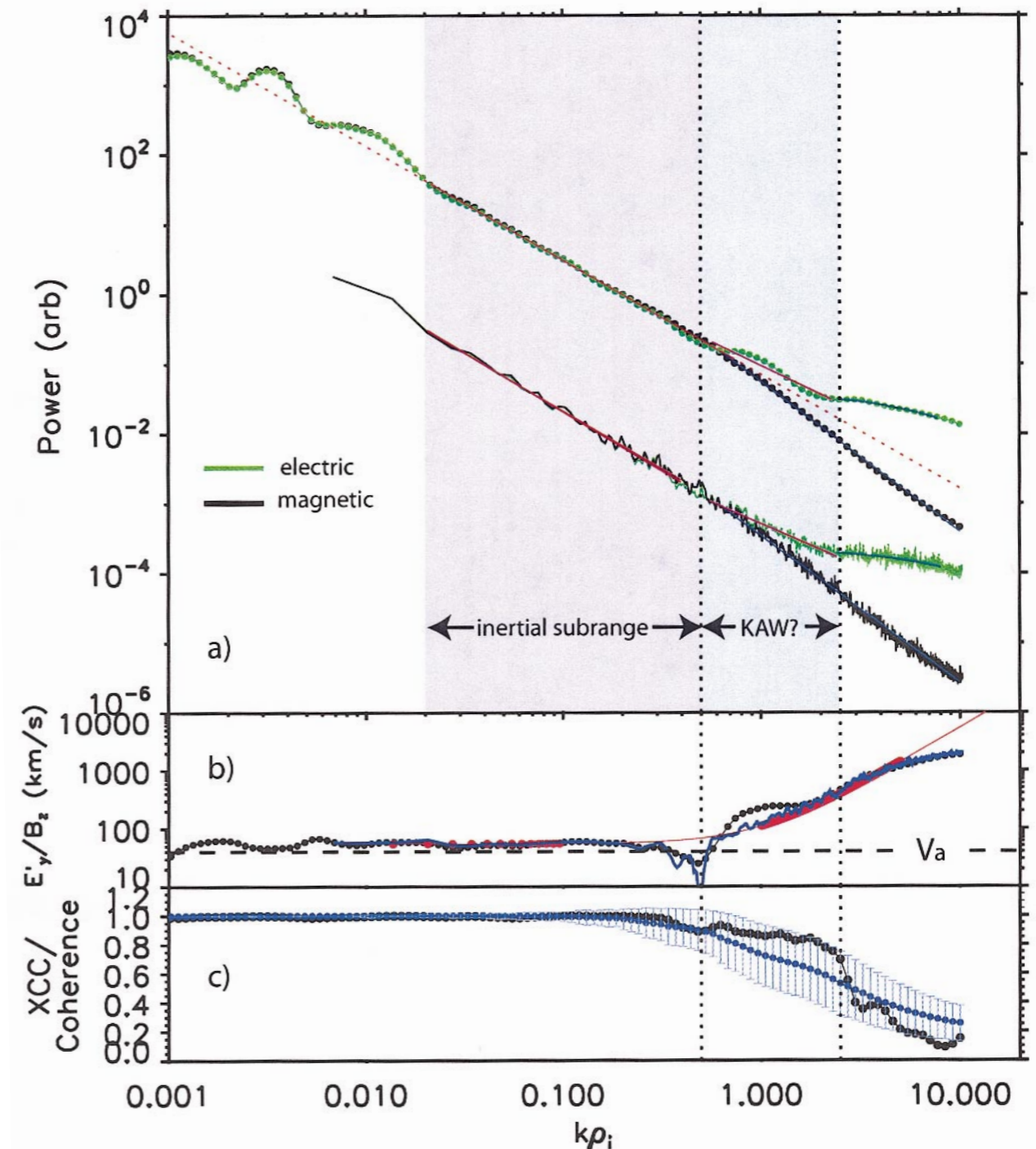


# Evidence for a KAW/perpendicular cascade

- Cluster measurements of the electric field of solar wind turbulence show that:
  - the cascade is Alfvénic - E and B are strongly correlated
  - the short wavelength electric field power is enhanced
  - the E/B ratio is consistent with Alfvénic inertial range and evolution to kinetic Alfvén waves at short wavelengths
  - density spectrum is  $k^{-5/3}$

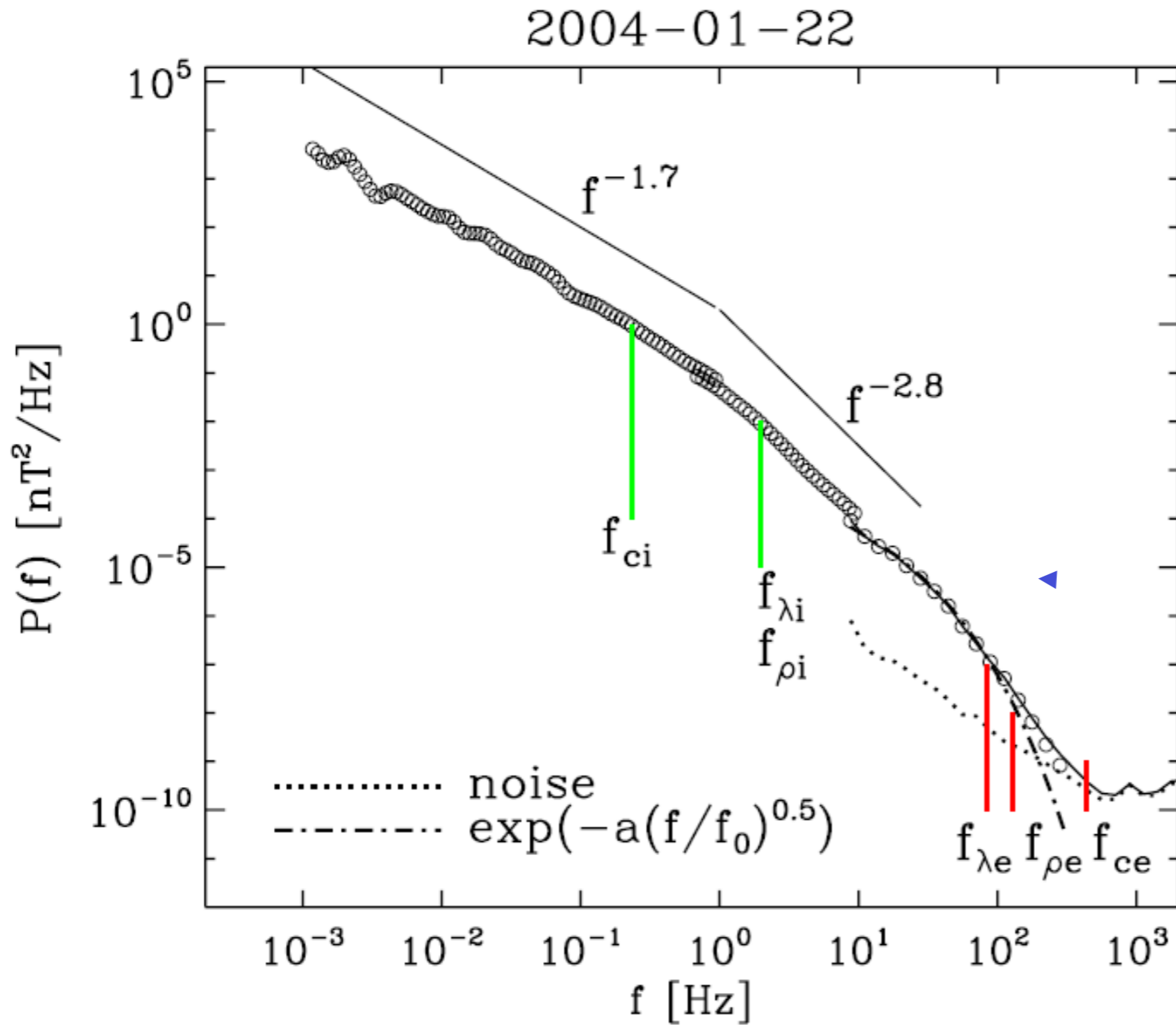
## Caveats:

- Cluster is only in the solar wind for short intervals
- Spin tones (more later...)
- EFW noise levels and sampling rates



(Bale et al, 2005)

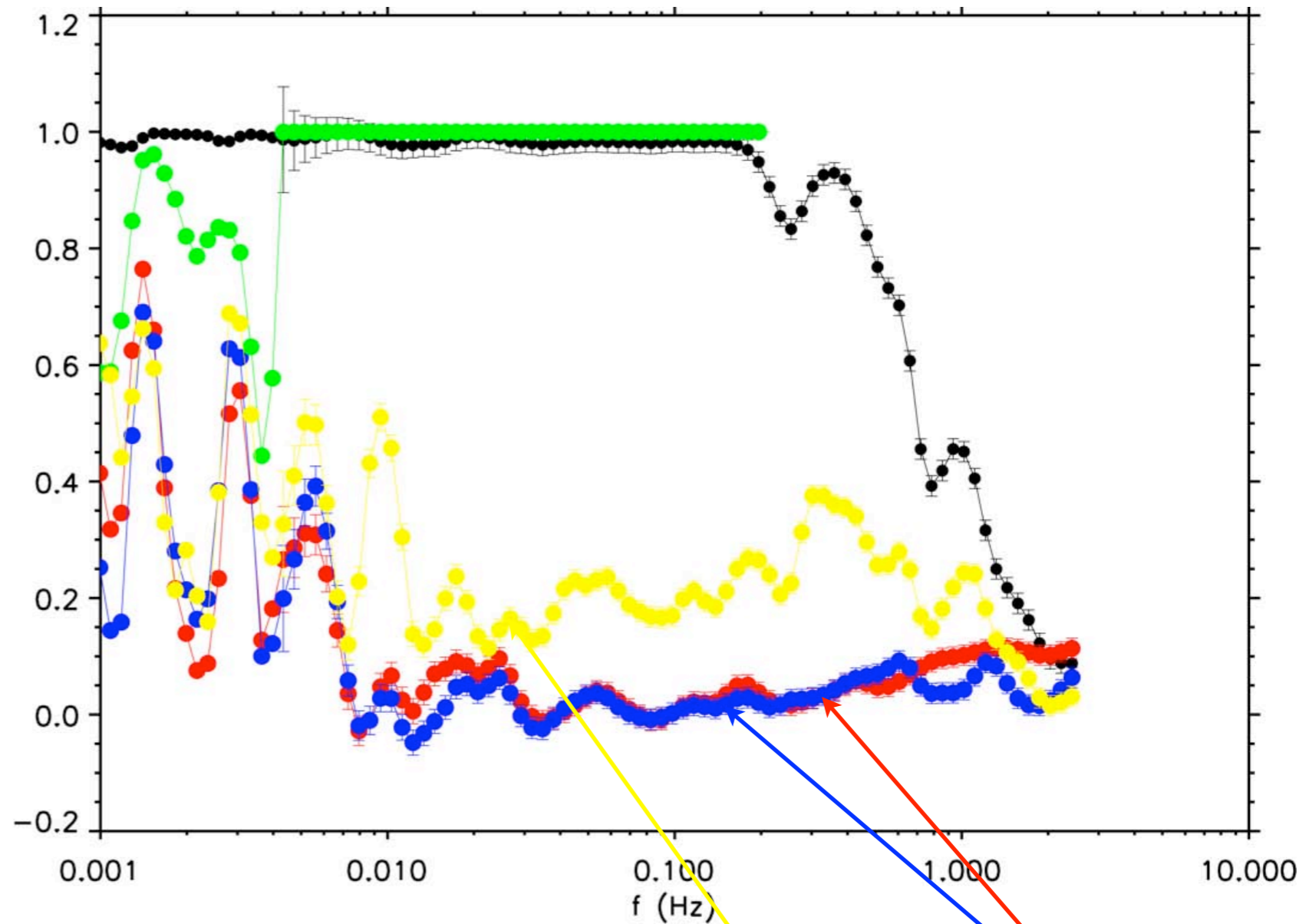
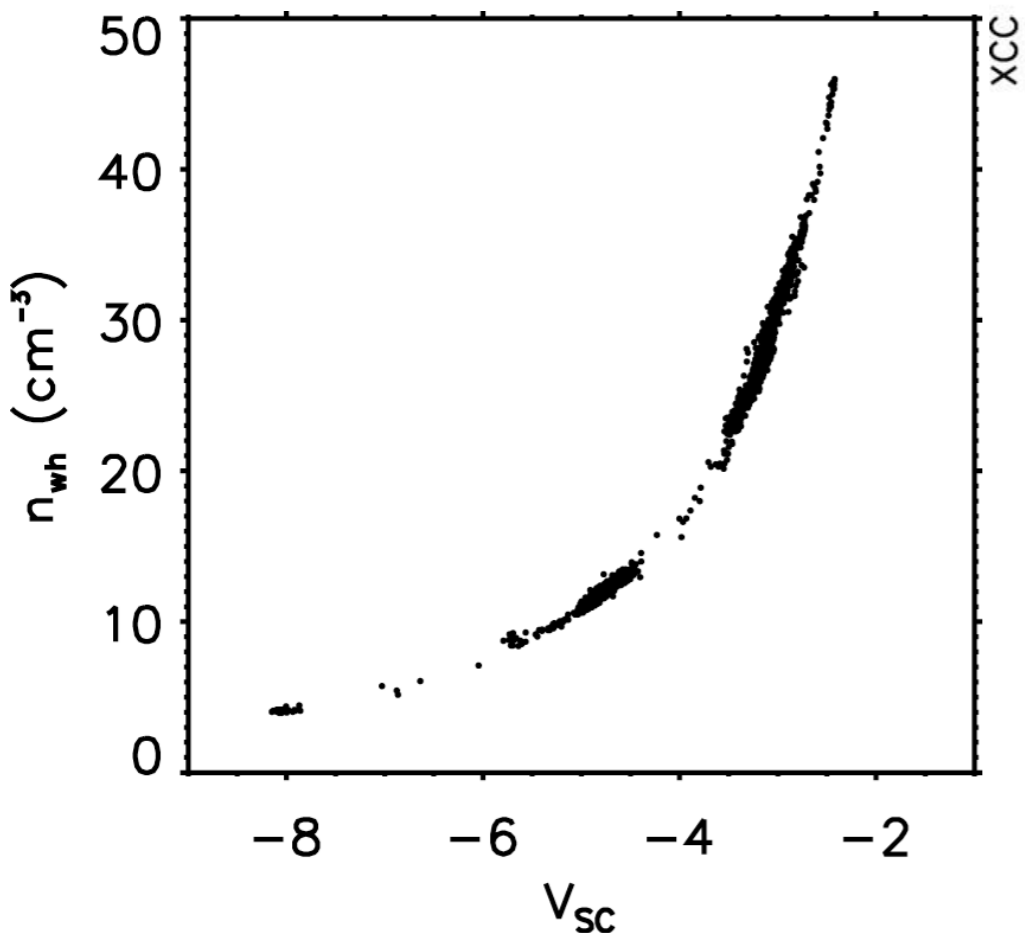
# Magnetic turbulence in the Solar Wind : Evidence for slope break in the electron range



Alexandrova et al.,  
PRL, 2009

# Evidence for a perpendicular cascade

Measurements of spacecraft potential can be calibrated to give density (locally)

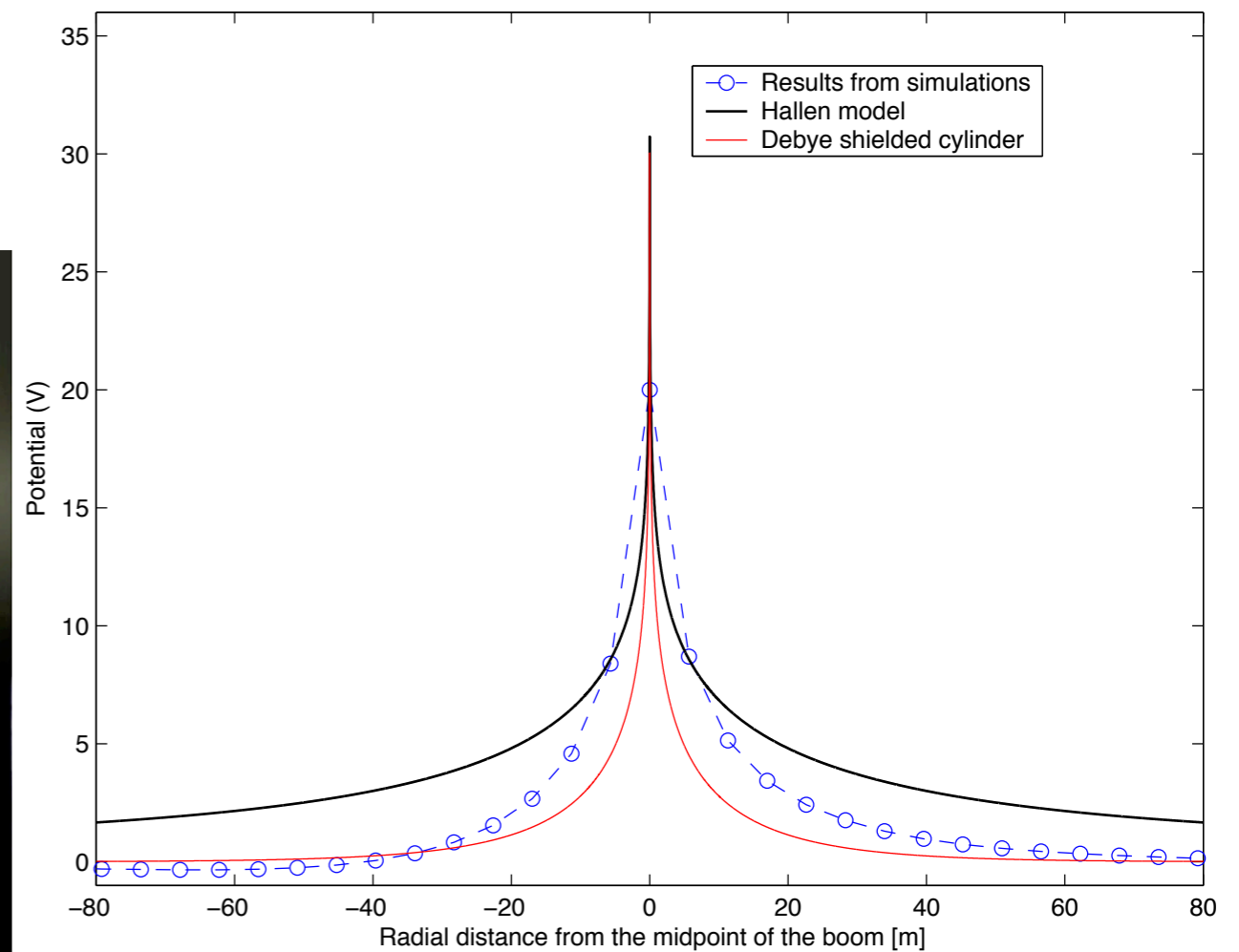
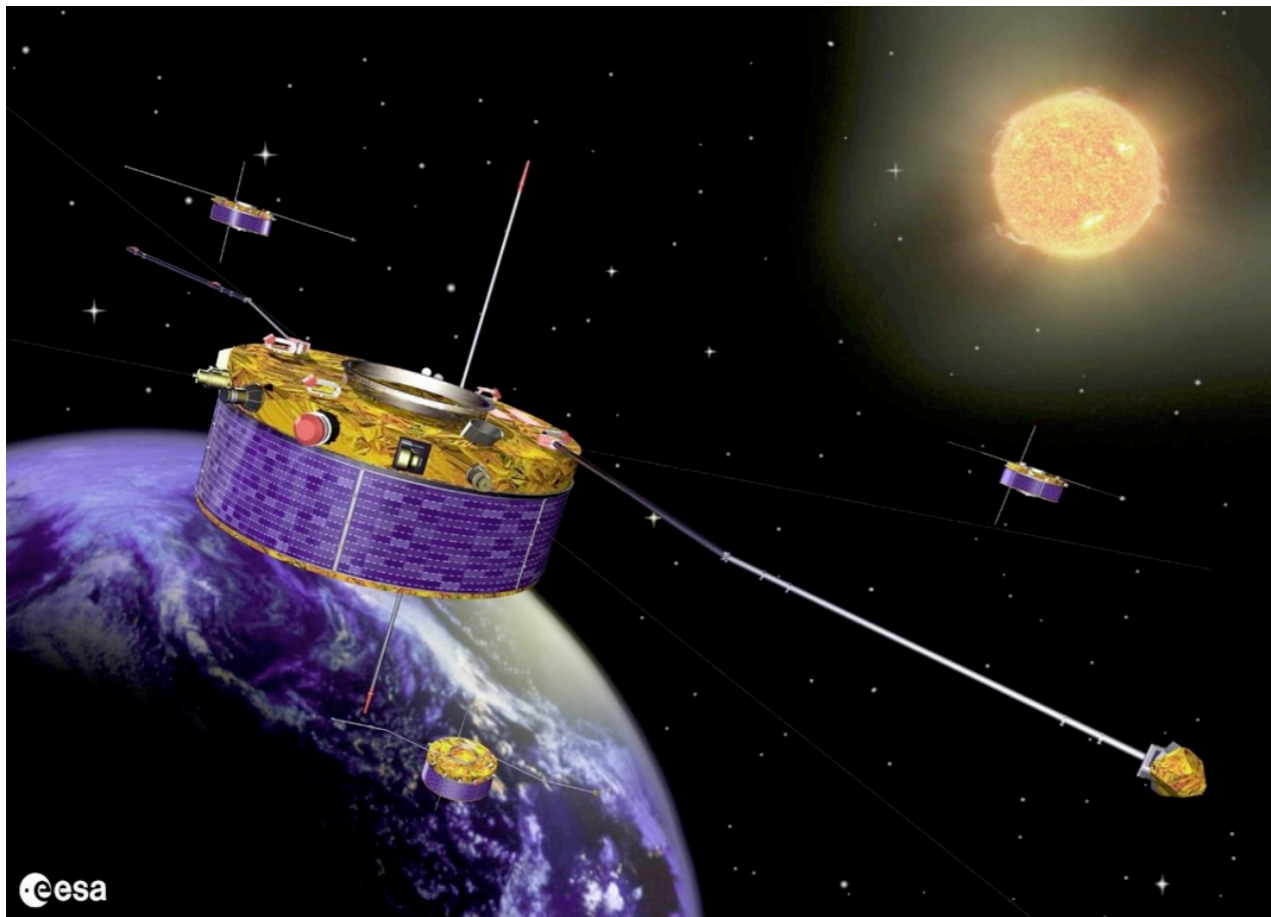


cross-correlation of density and fields

Density and fields are poorly correlated - **not much compressive power!**

# Electric field measurements

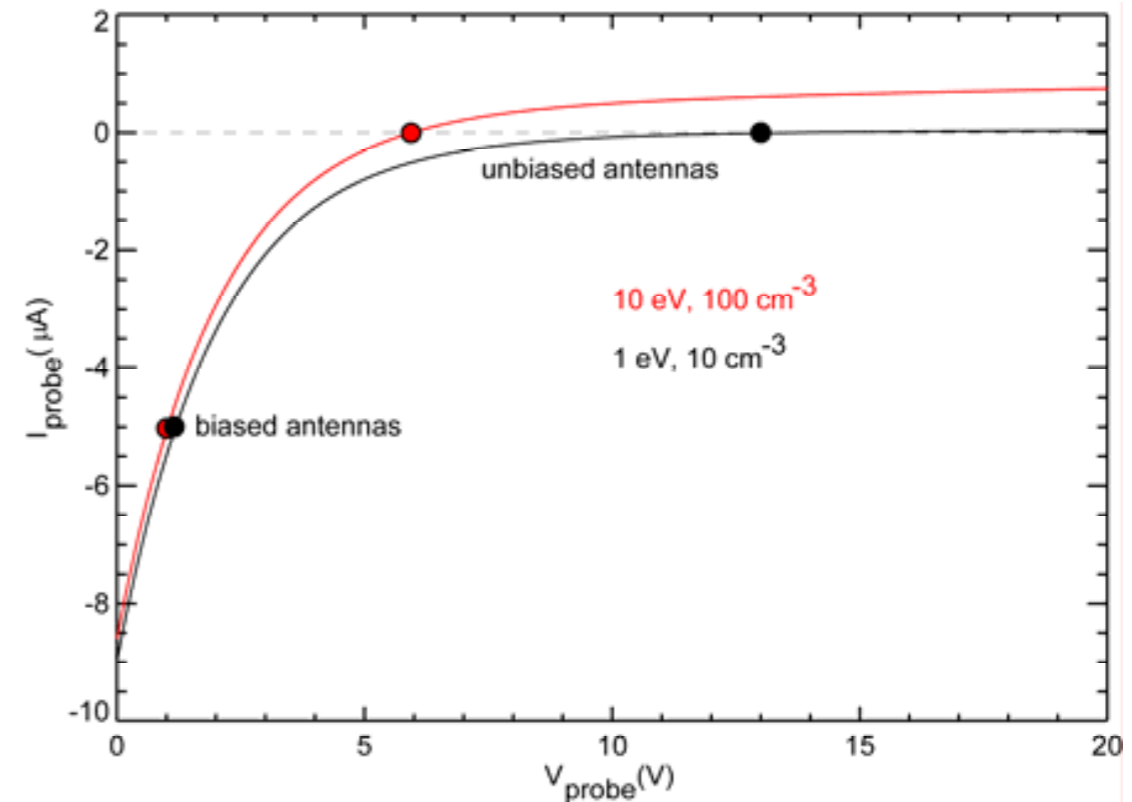
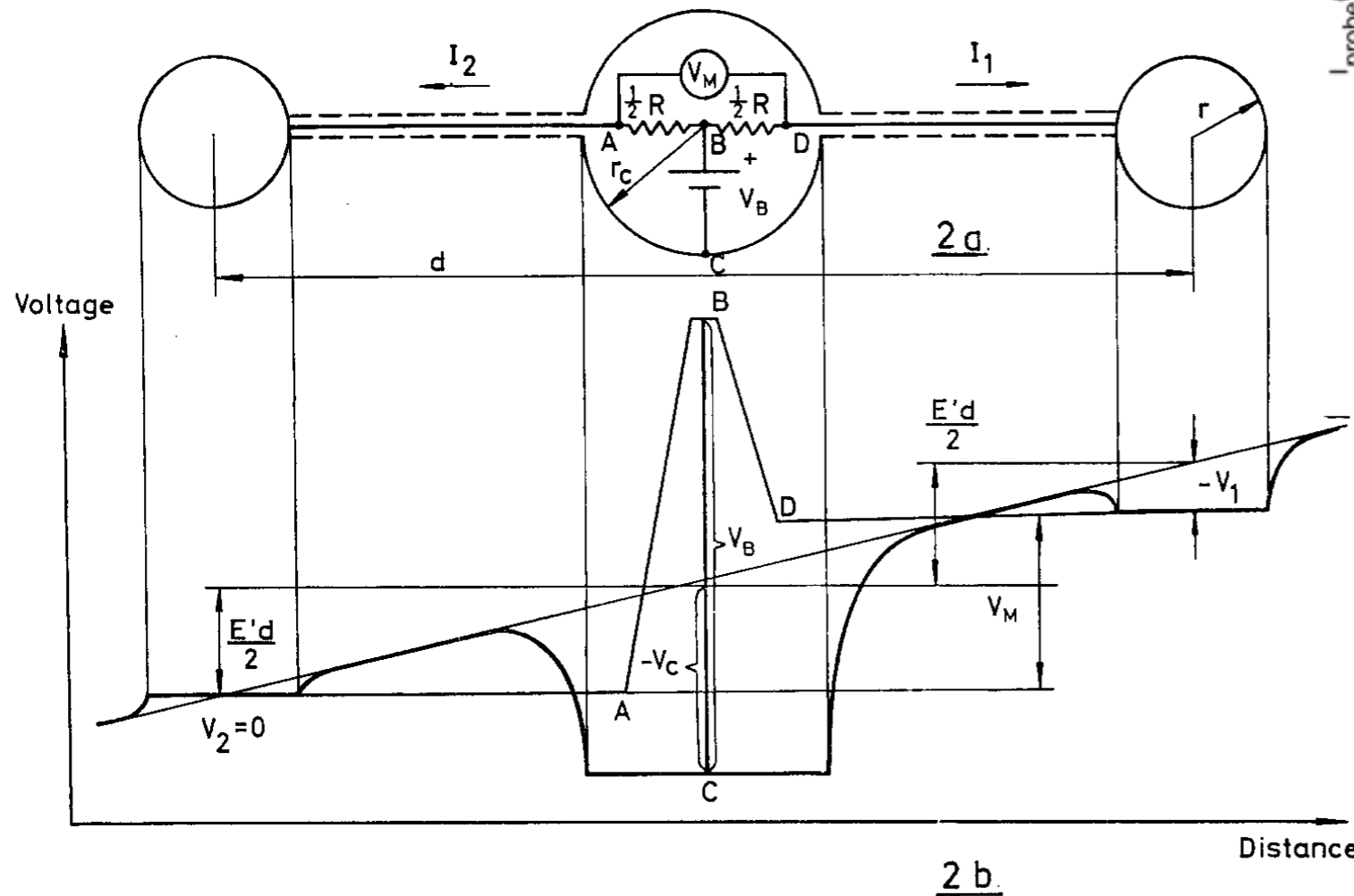
- Voltage probes (and spacecraft) are Langmuir probes
- Current balance (thermal, photoelectron, secondaries) determines floating voltage



Cluster (and THEMIS) satellites have double-probe measurements, but ecliptic plane wire booms spin through the plasma wake (and have large photoelectron variations)

# Electric field measurements

- Voltage probes (and spacecraft) are Langmuir probes
- Current balance (thermal, photoelectron, secondaries) determine floating voltage



- Bias current minimizes voltage variations due to natural currents
- Unbiased probes measure primarily current variations - this is historically the case for SW experiments

Fig. 2. Three-electrode probe system. Potential along a line in the plasma through the probes and along a line through the lead  $ABD$ .

(Fahleson)

# LF/DC electric field measurements

Good LF gain requires that we **maximize** the base resistance  $R_B$  or **minimize or control**  $R_S$

$$G_{LF} \approx \frac{R_B}{R_S + R_B}$$

in shadow  $R_S \sim T_e/j_p$  which is highly variable

in sunlight  $R_S \sim V_p/(j_e + j_{bias})$  which is smaller, less variable, and easier to control

to make  $R_b$  large, minimize electron exchange between the spacecraft and sensors

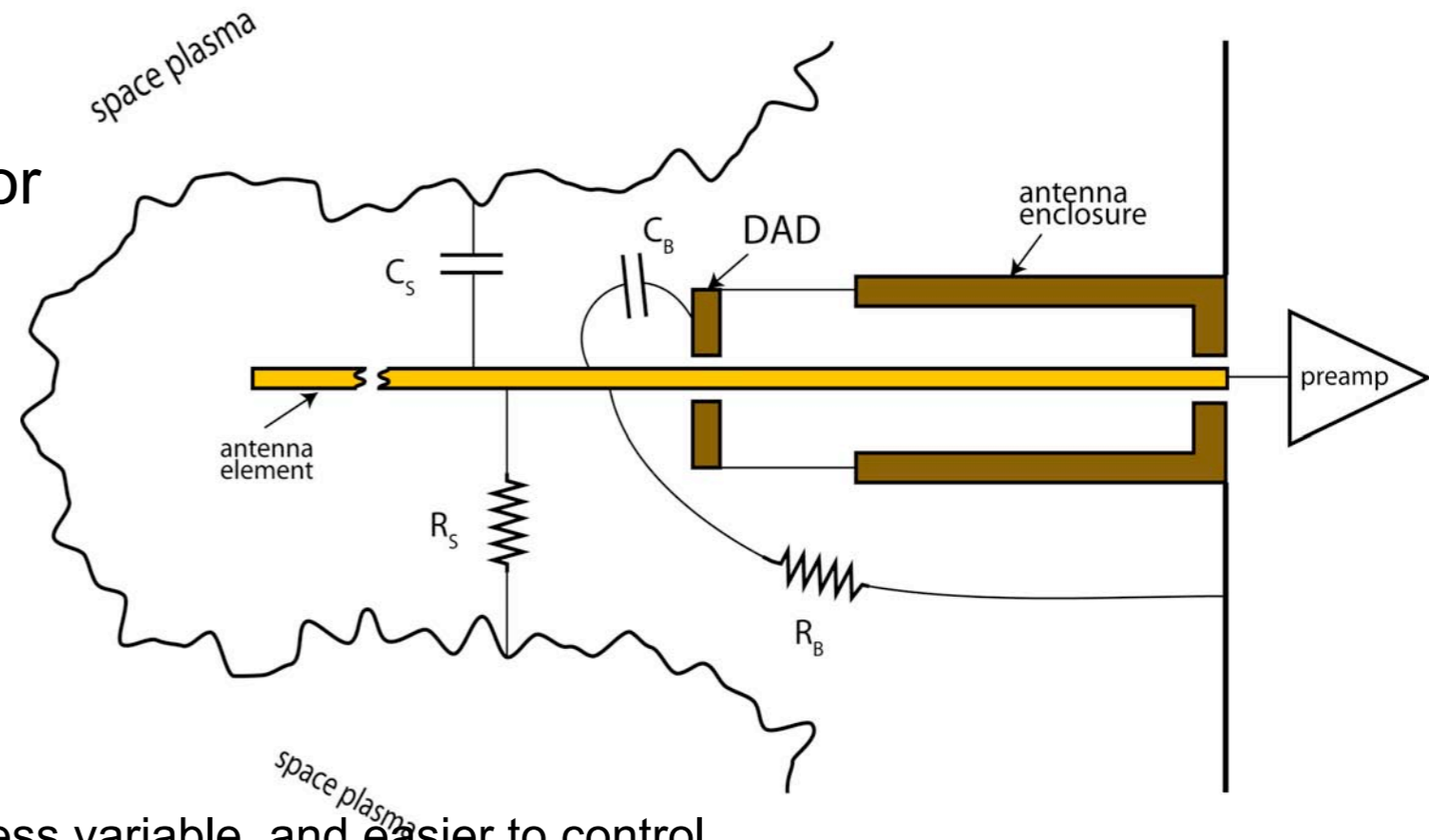
put sensors far from spacecraft (ie. sensors at the end of booms)

put up a voltage barrier (voltage 'guard' surfaces)

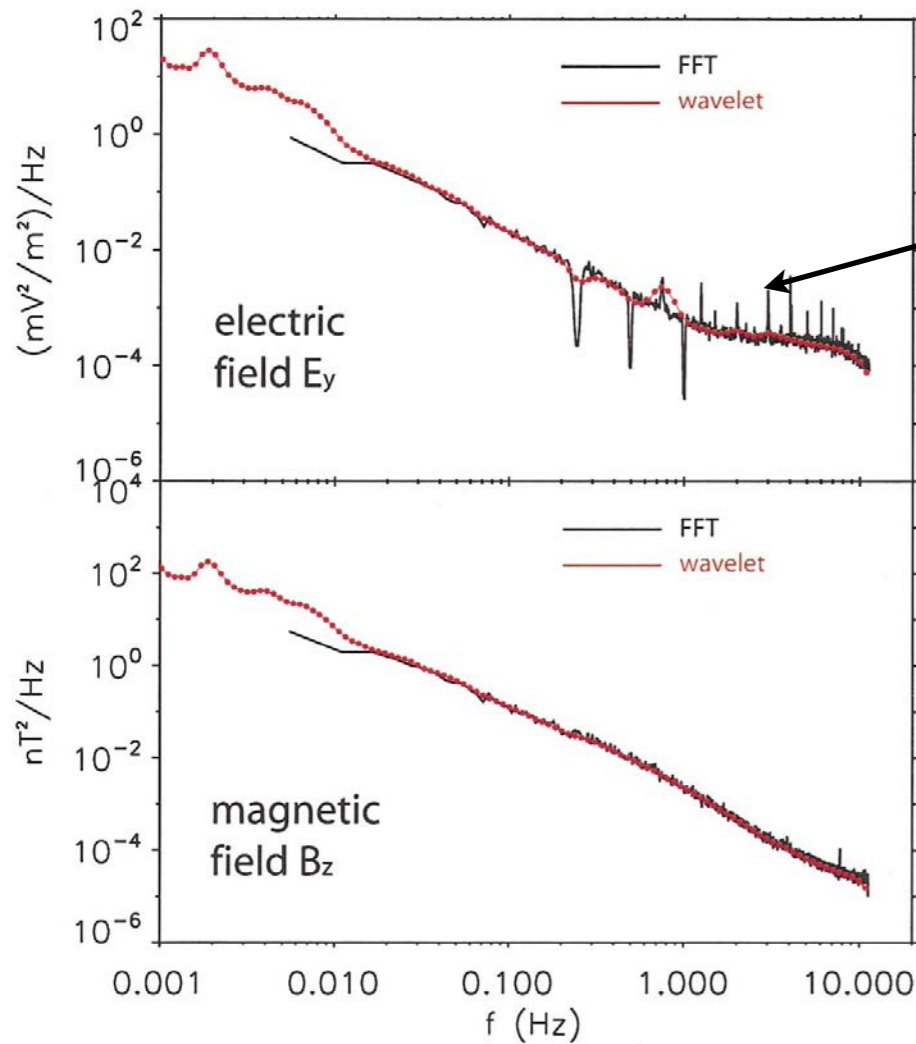
sensors are acting as Langmuir probes - put them as CLOSE as possible to each other on the I-V curve

-  $R_s$  and  $R_b$  should be same for each antenna - **symmetry w.r.t the Sun is critical!**

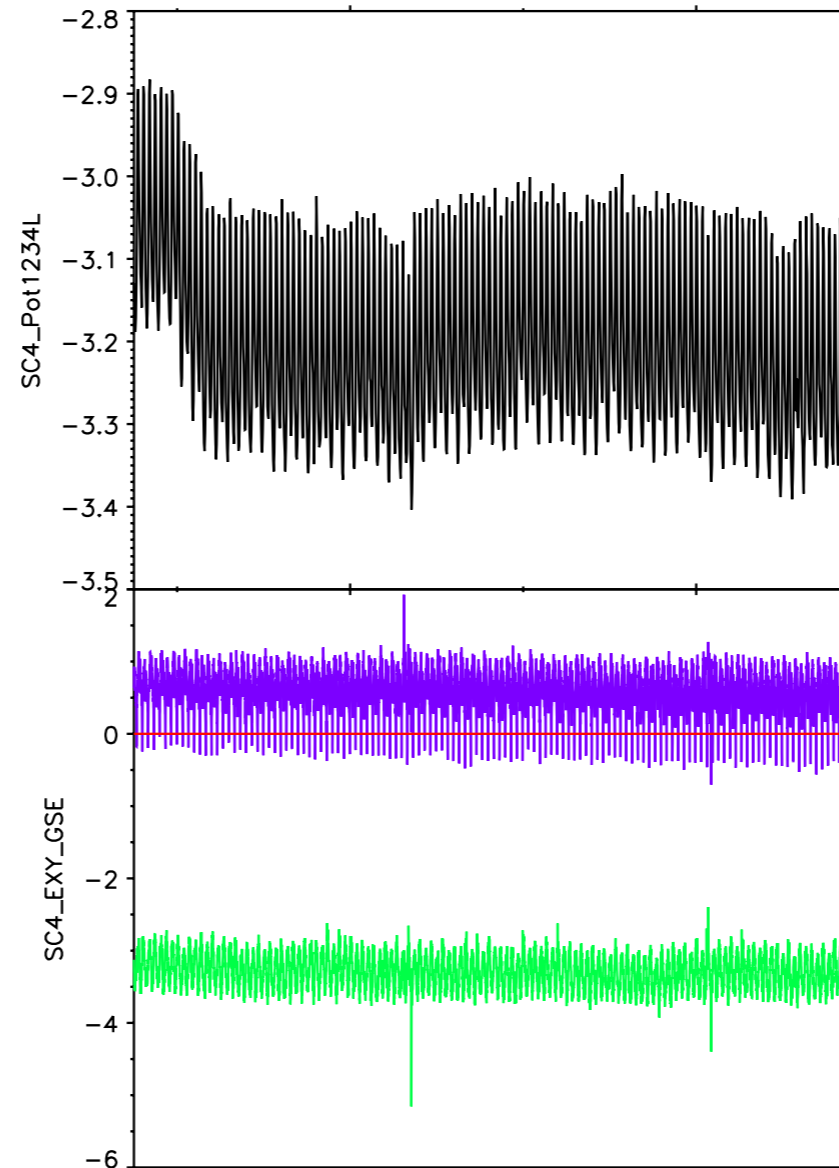
**summary:** antennas *in sunlight* with *good symmetry* and *away from the wake* and shorter  $\lambda_D$  allows the measurement of DC/LF electric field



# Electric field measurements in the solar wind



- Longer booms are better (for SNR), however spin-tones occur in the most interesting frequency range!
- Minimize variations in solar illumination



raw voltage data with spin tone

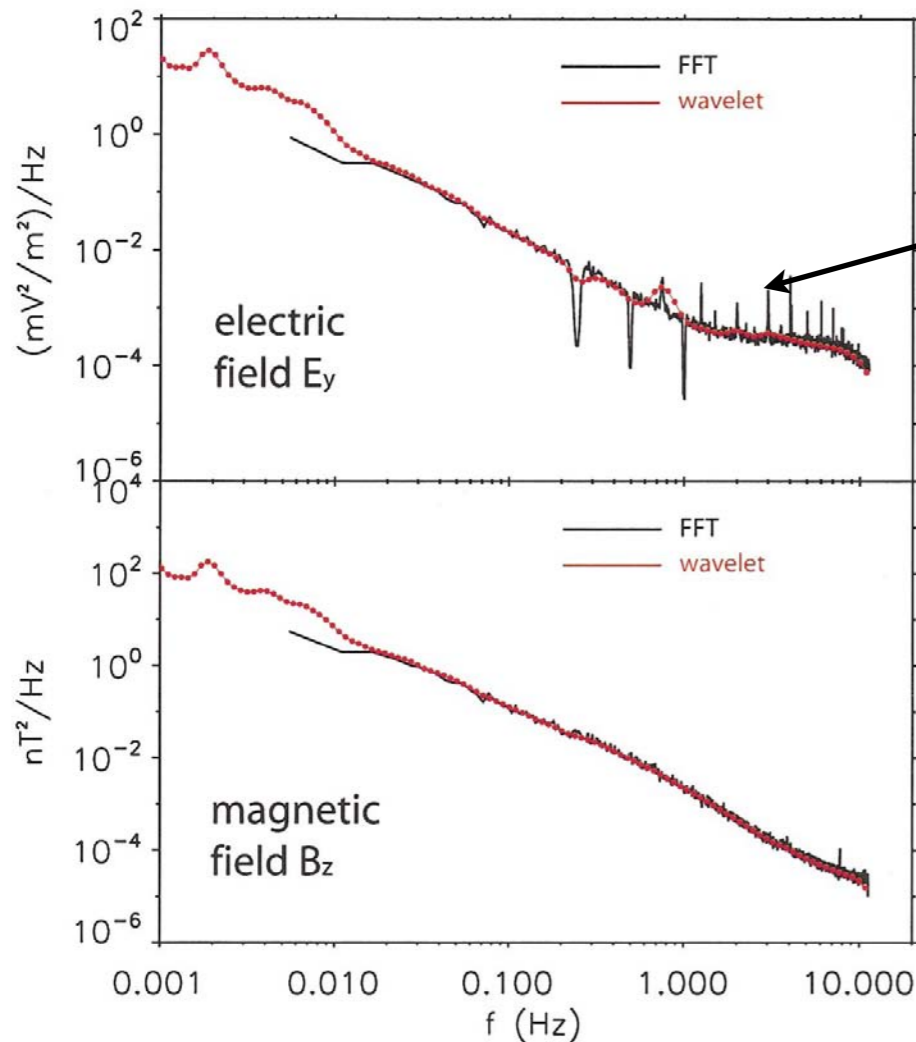
hhmm  
2002 Feb 19

0038

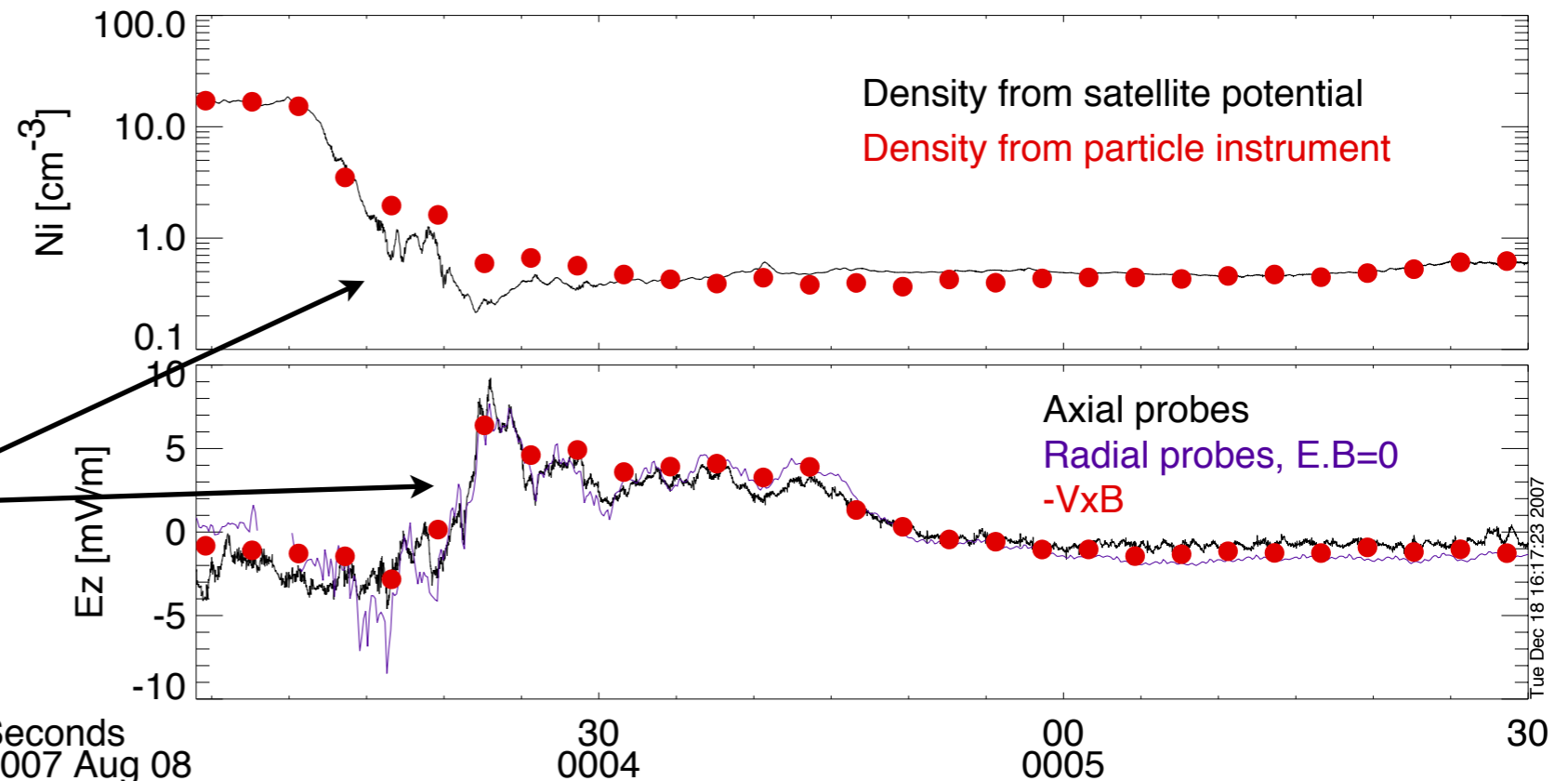
0040



# Electric field measurements in the solar wind



- Longer booms are better (for SNR), however spin-tones occur in the most interesting frequency range!
- Minimize variations in solar illumination



- Short axial booms can do pretty well, especially when  $\lambda_D$  is small

# Magnetic field measurements

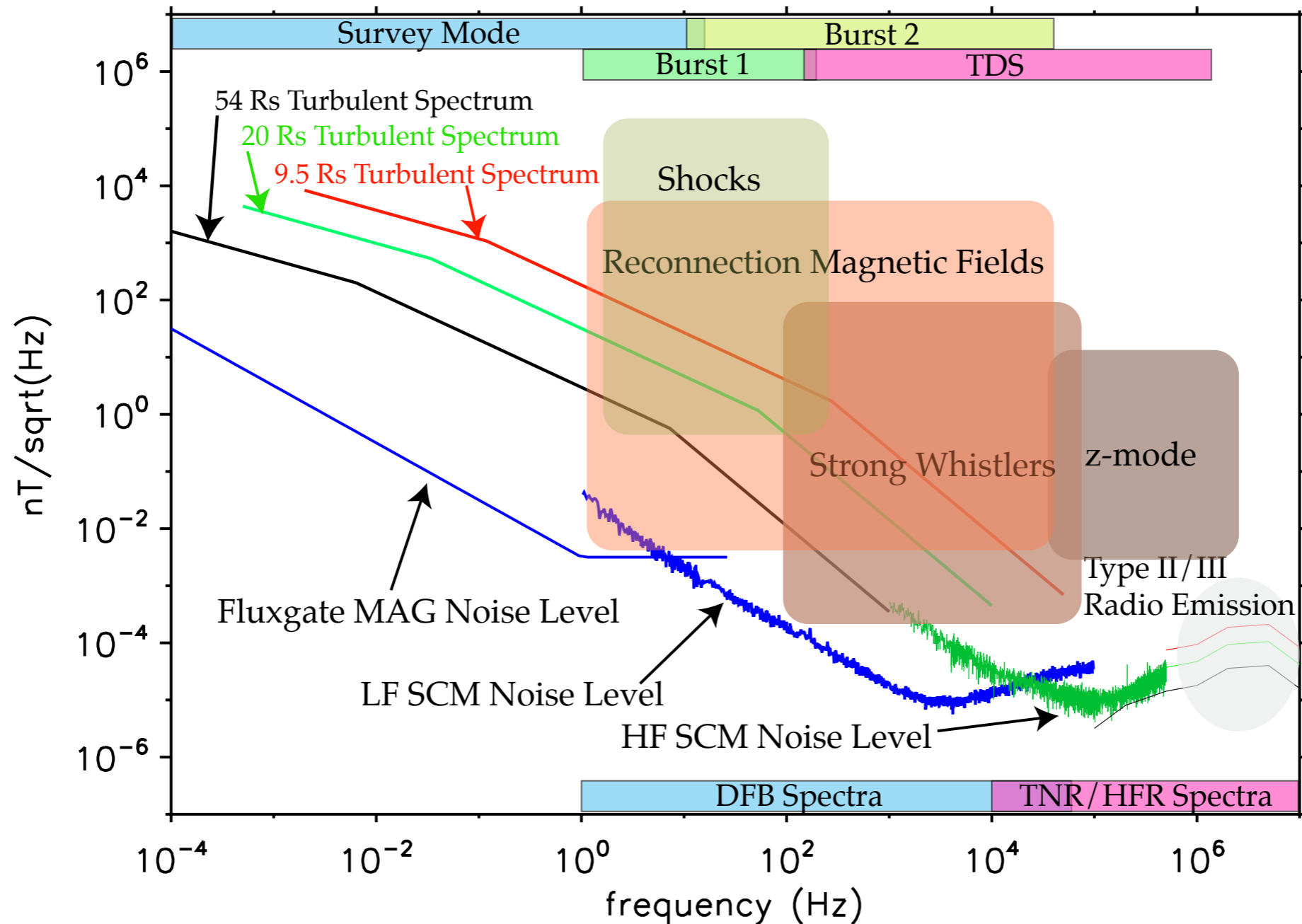
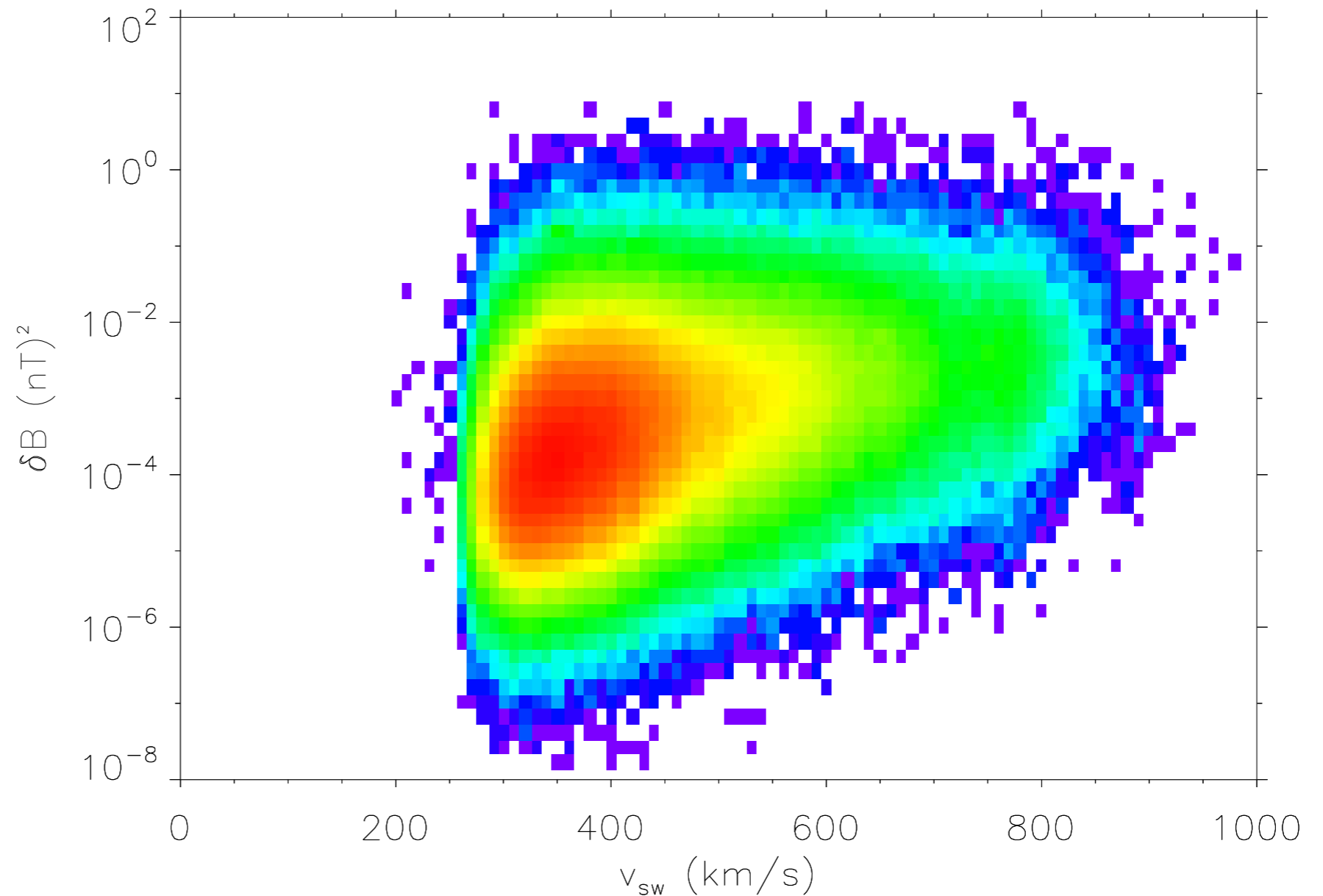


**Figure D.2-6.** Sensitivity of magnetic field and waves measurements. The SCM and MAG together cover the full range of required measurements. SCM becomes more sensitive than MAG at  $\sim 10$  Hz. The HF SCM measures z-mode, very intense radio bursts, and very fast solitary waves.

# $\delta B^2$ vs solar wind speed

---

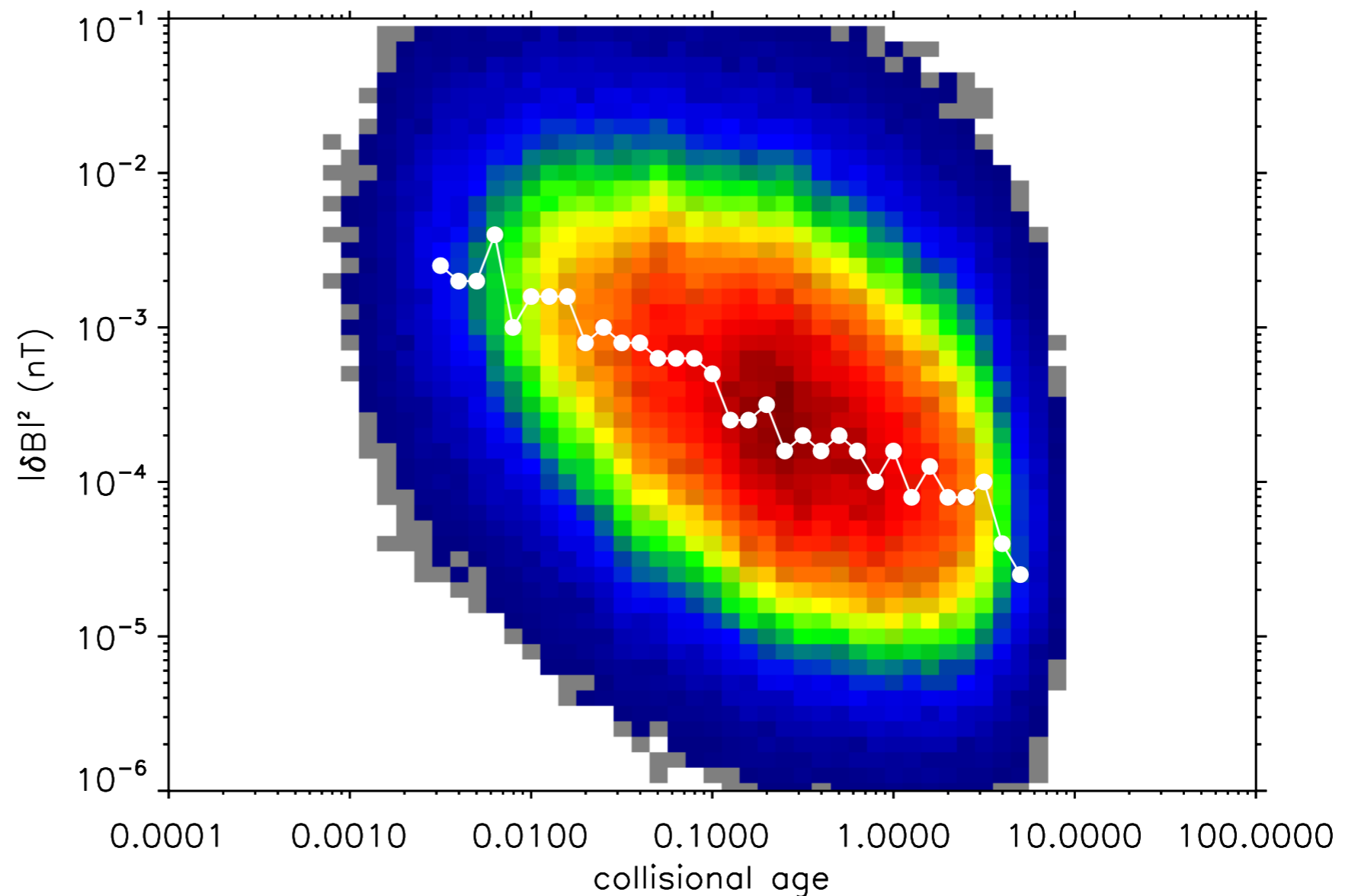
high speed wind has larger magnetic fluctuation levels  $\delta B$  - this is well known  
- is there something special about the source?



# $\delta B^2$ vs collisional age

on the other hand, 'age' =  $\nu R/v_{sw}$  is a measure of the number of Coulomb collisions since leaving the Sun. So maybe it's not the source (alone) but rather the local evolution

More 'active'  
plasma is more  
collisionless



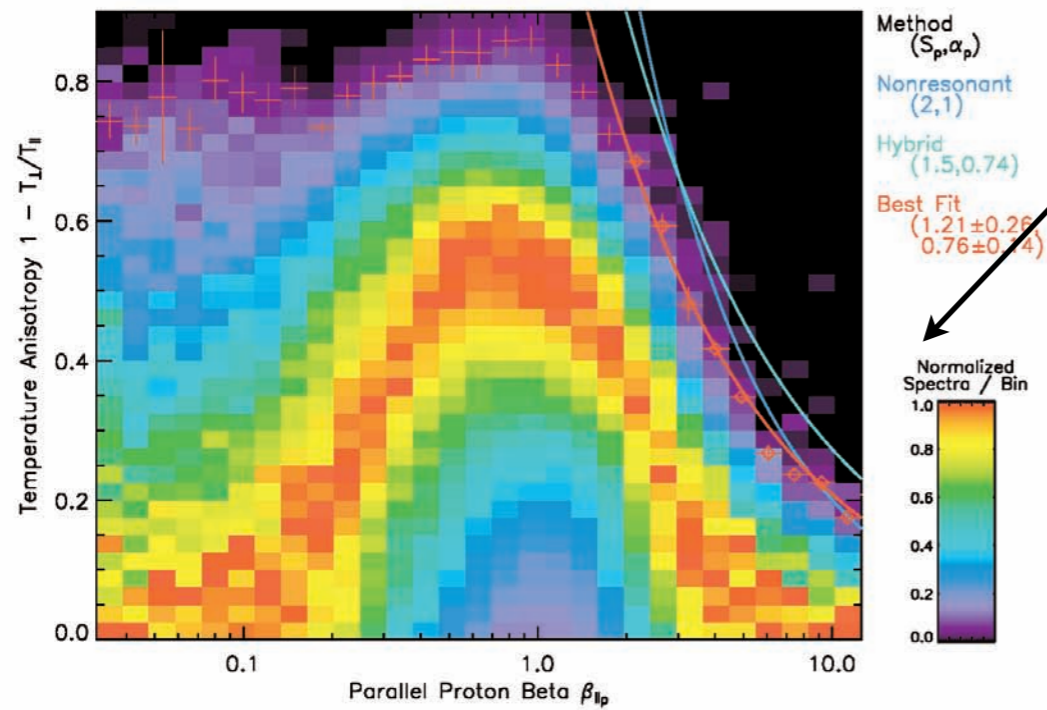
# Local instabilities inject power directly at small scales

---

- Ion pressure anisotropy instabilities
  - Mirror and/or AIC for  $T_{\perp}/T_{\parallel} > 1$
  - Firehose for  $T_{\perp}/T_{\parallel} < 1$
- Electron pressure anisotropy instabilities
- Streaming instabilities
  - proton-proton
  - proton-alpha
- Heat flux instabilities
- Electron beam instabilities
  - Langmuir/beam mode generation at near  $f_{pe}$

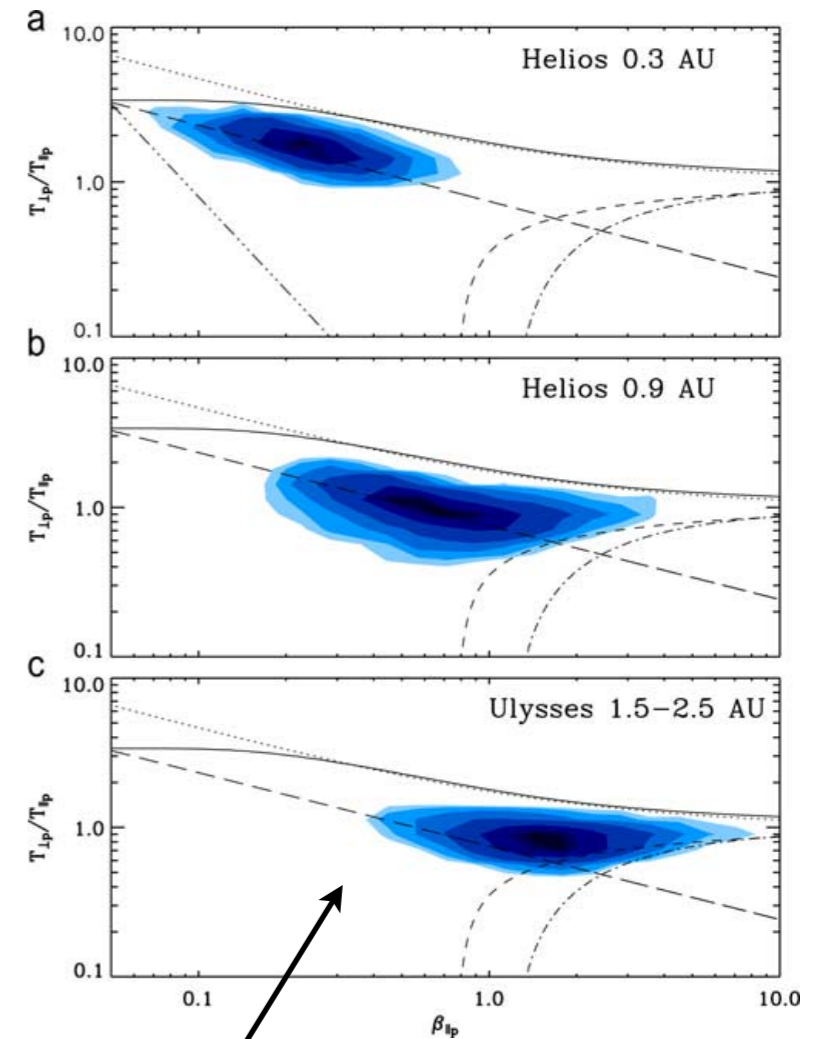
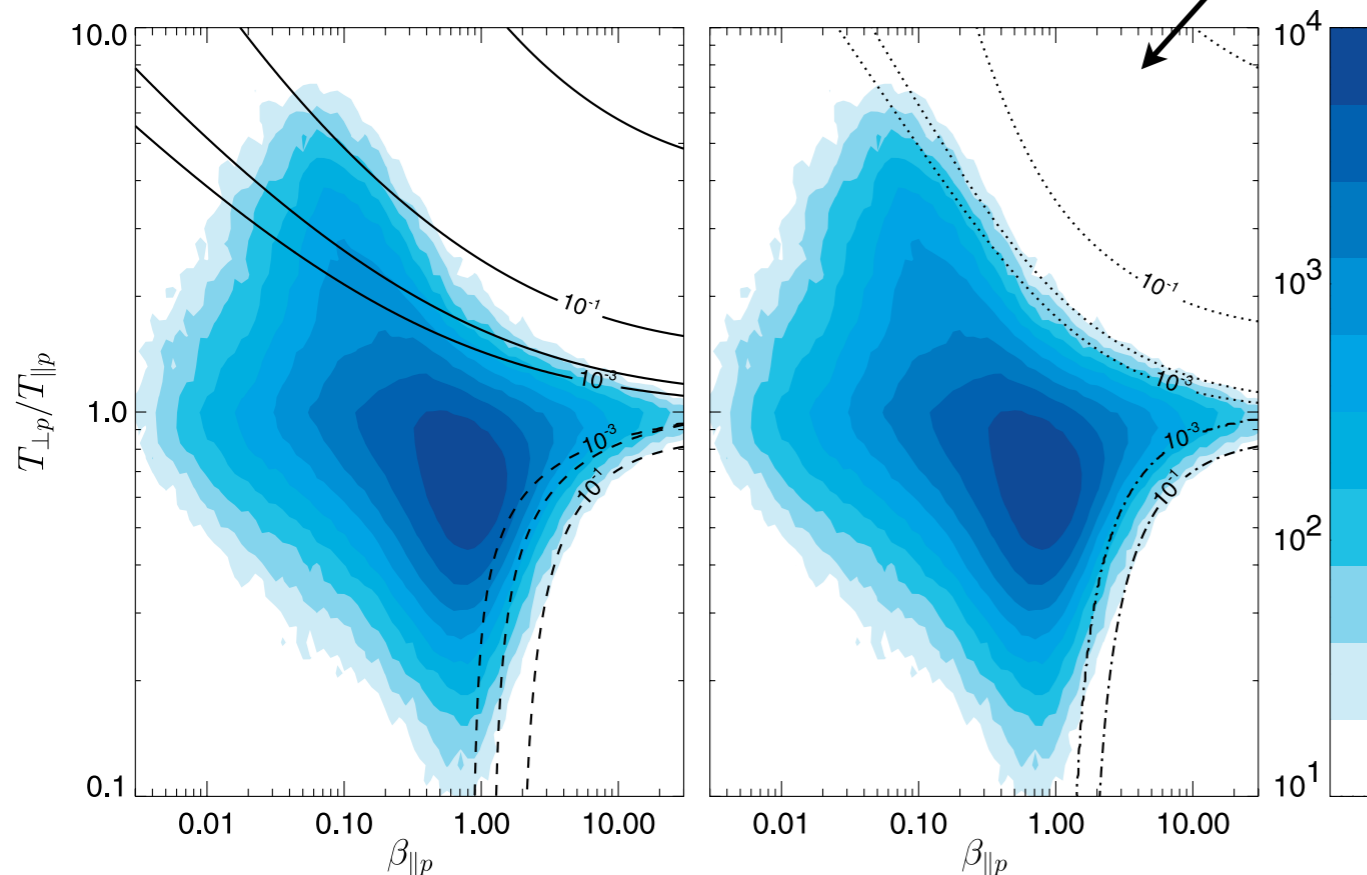
These instabilities will generate power at  $k\rho_i \sim 1$  or shorter

# Proton pressure anisotropy



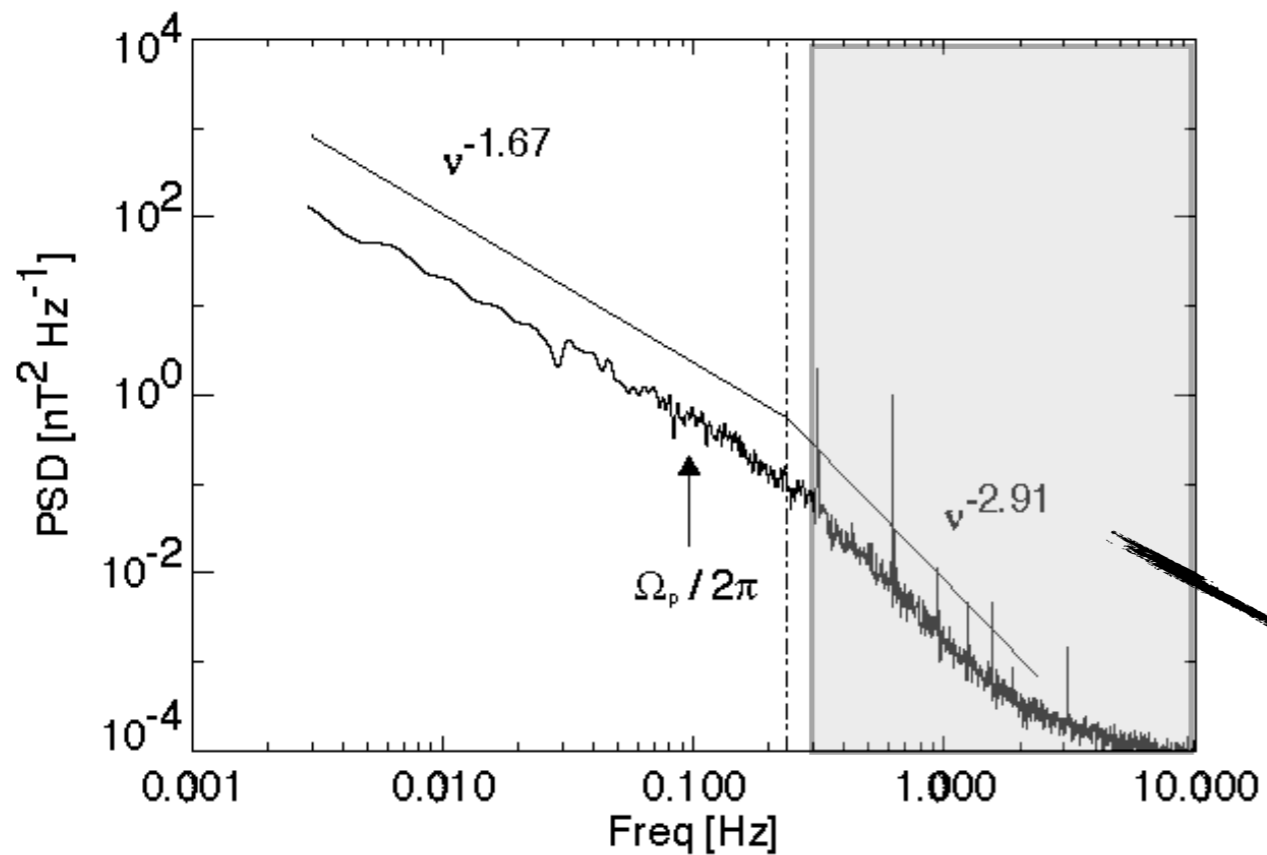
Firehose limits  
(Kasper et al, 2002)

Mirror, AIC, and  
oblique firehose  
(Hellinger et al, 2006)



Fast wind evolution  
and constraints  
(Matteini et al, 2007)

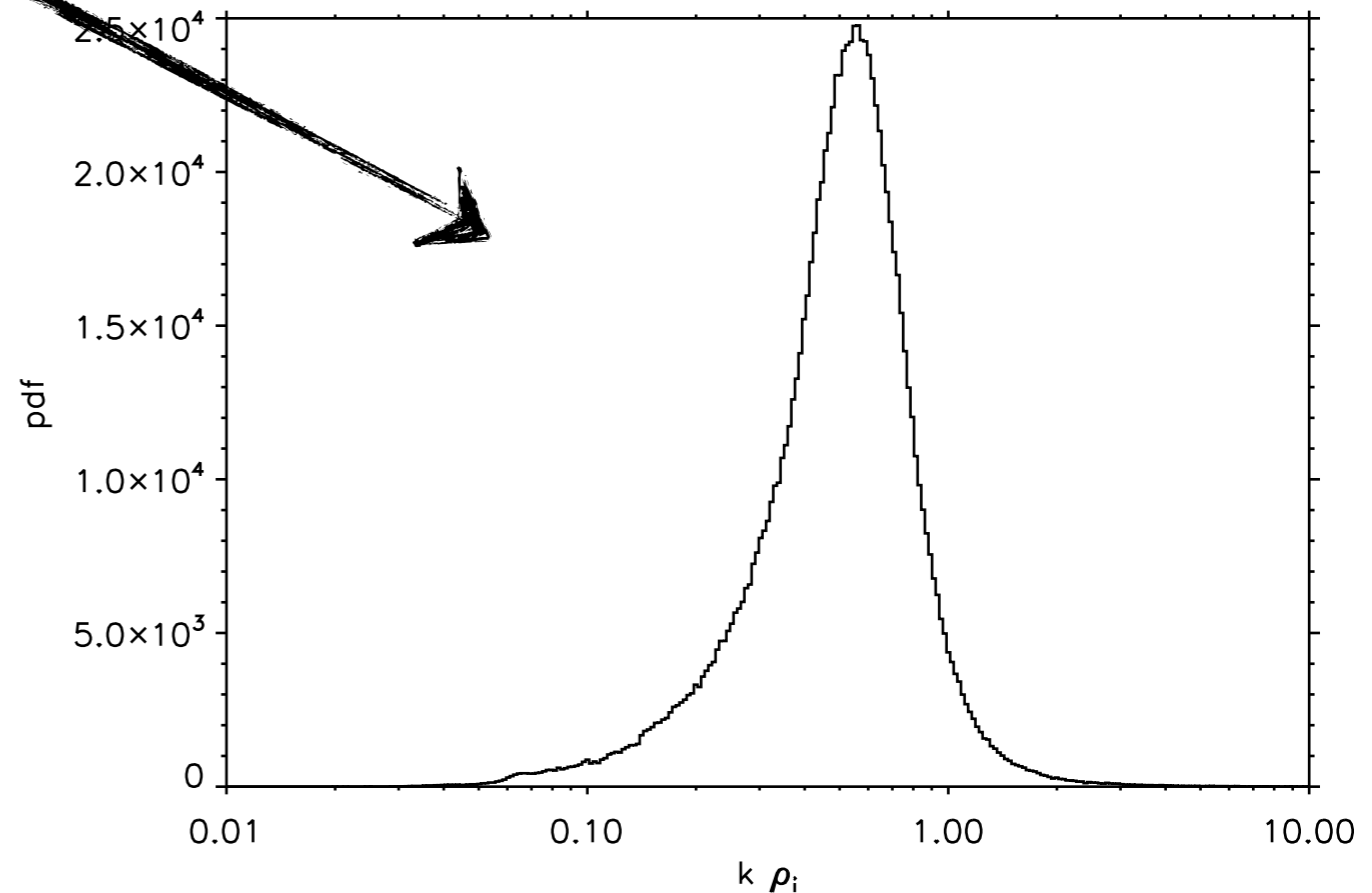
# WIND magnetic field data - bandwidth



(Leamon et al., 1998)

...corresponds to  $k\rho_i \sim 0.6$   
(in part, because  $T_p \sim v_{sw}^2$ )

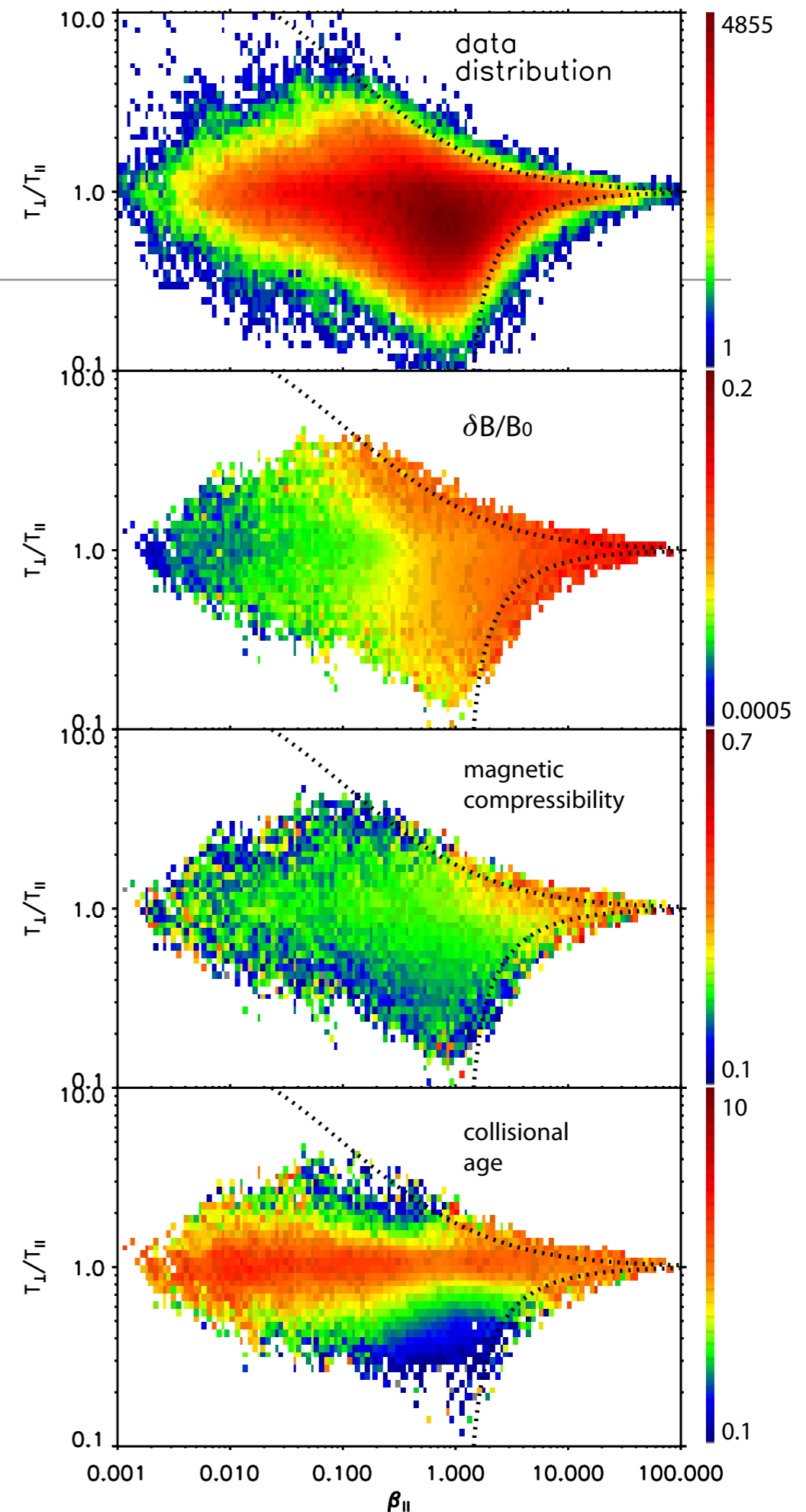
magnetic fluctuation data  
integrated over this band (3  
sec and faster)...



# Proton anisotropy instabilities

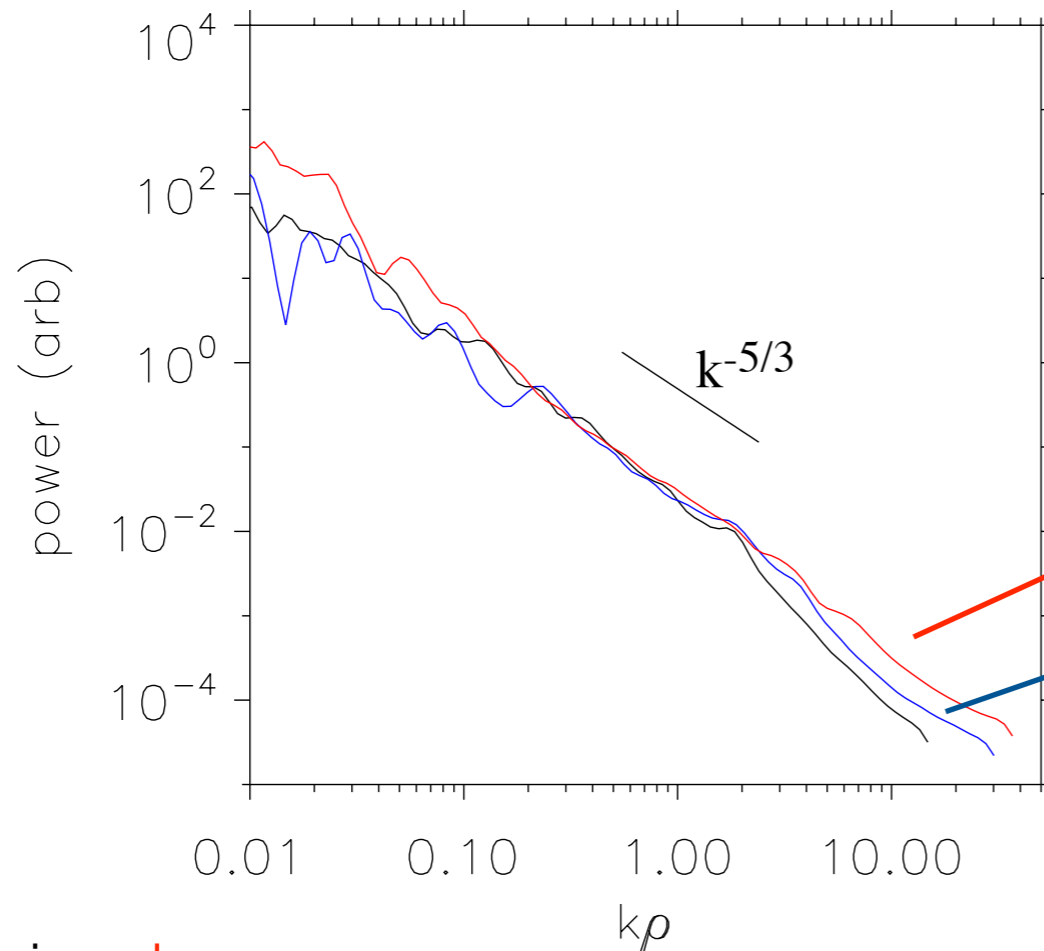
- Solar wind expansion and compression drive the proton distributions towards pressure-anisotropy instability thresholds
  1. Alfvén/Ion-cyclotron
  2. Mirror mode
  3. Oblique firehose instability
- Wind measurements show  $\delta B$  fluctuations associated with instability thresholds, suggest mirror and oblique firehose (no  $\delta E$  measurements!)
- These instabilities inject fluctuation power directly at  $k\rho \sim 1$  (in contrast to the turbulent cascade)

(Bale et al., 2009)

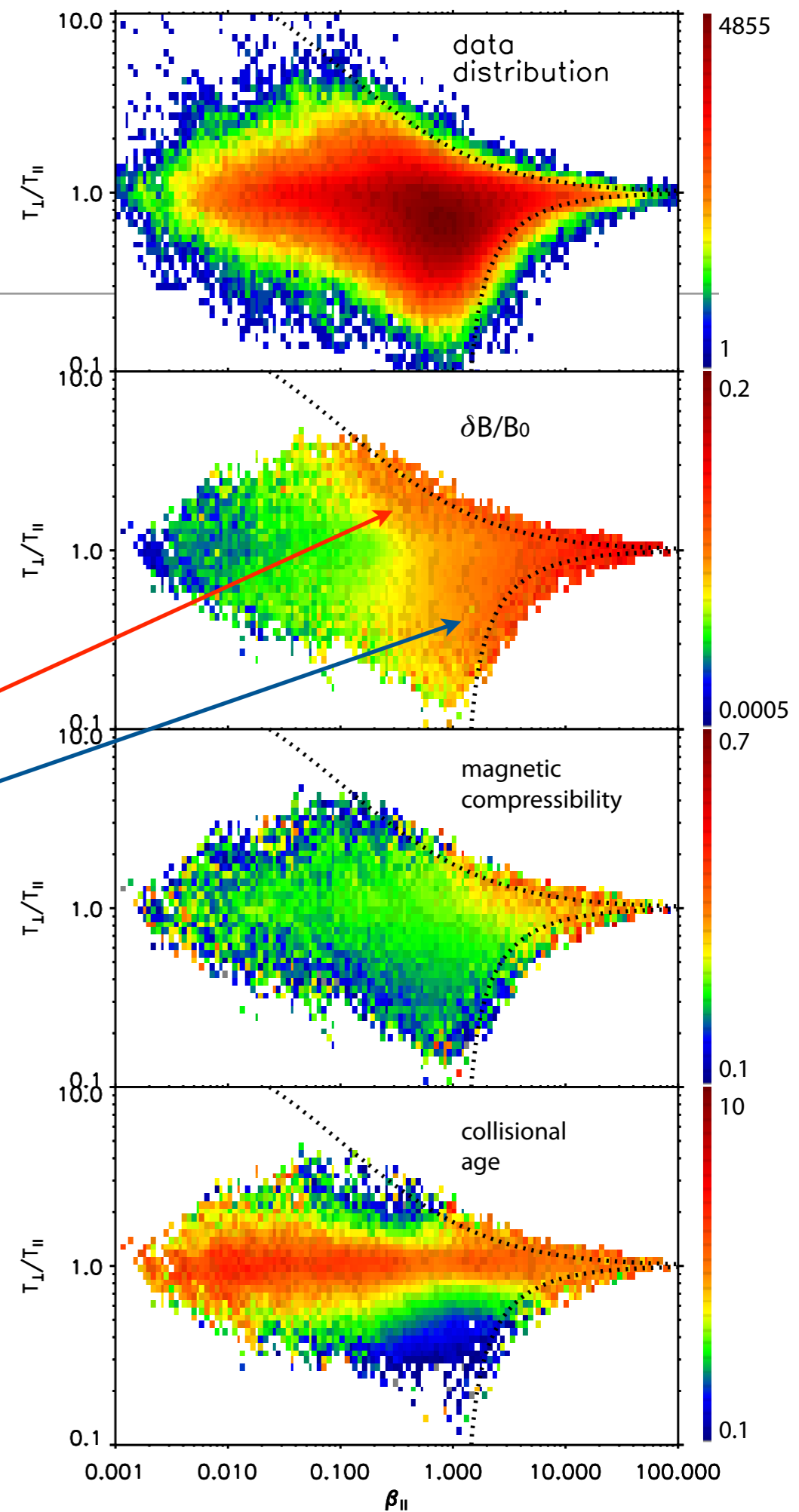




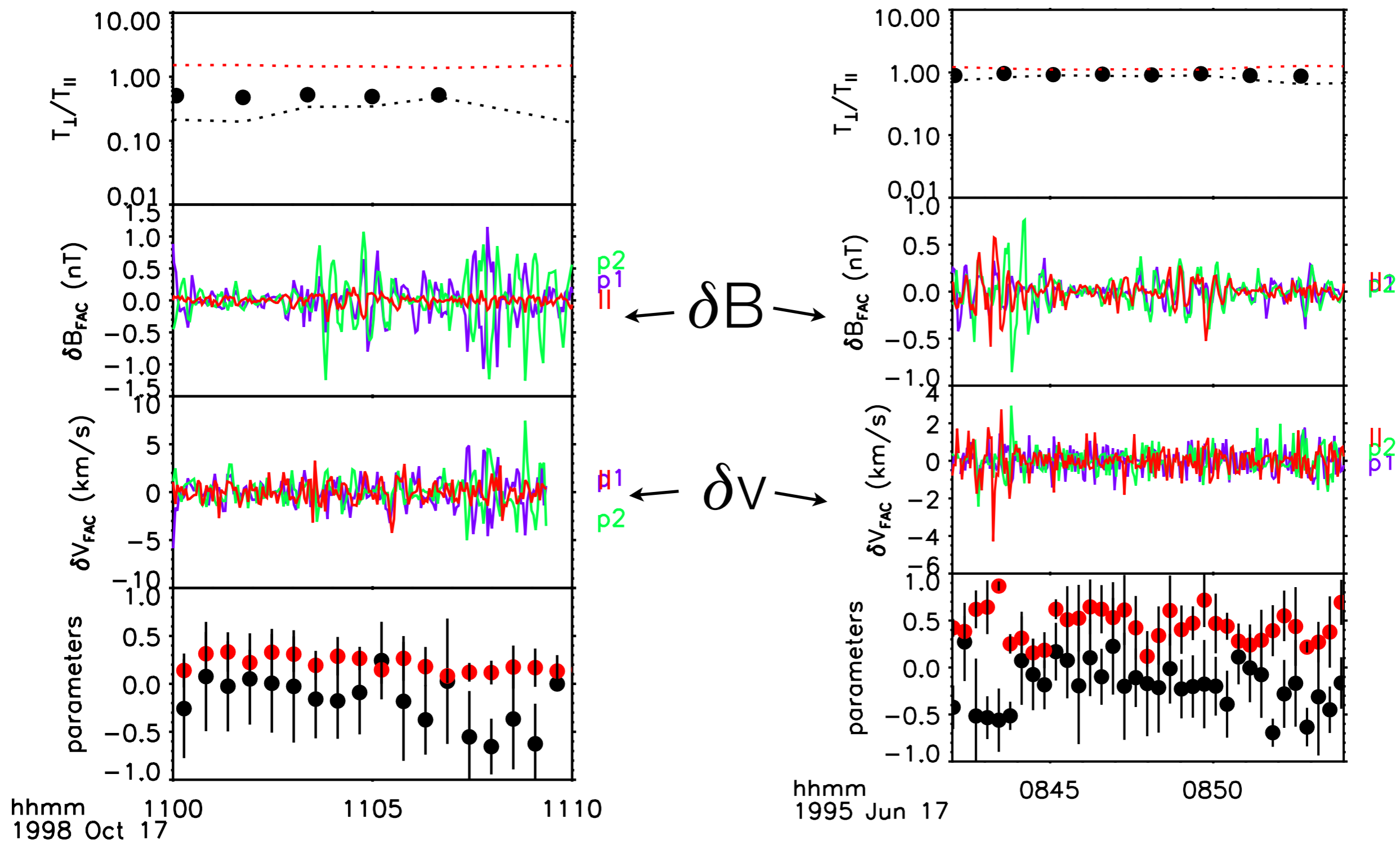
# Proton anisotropy instabilities



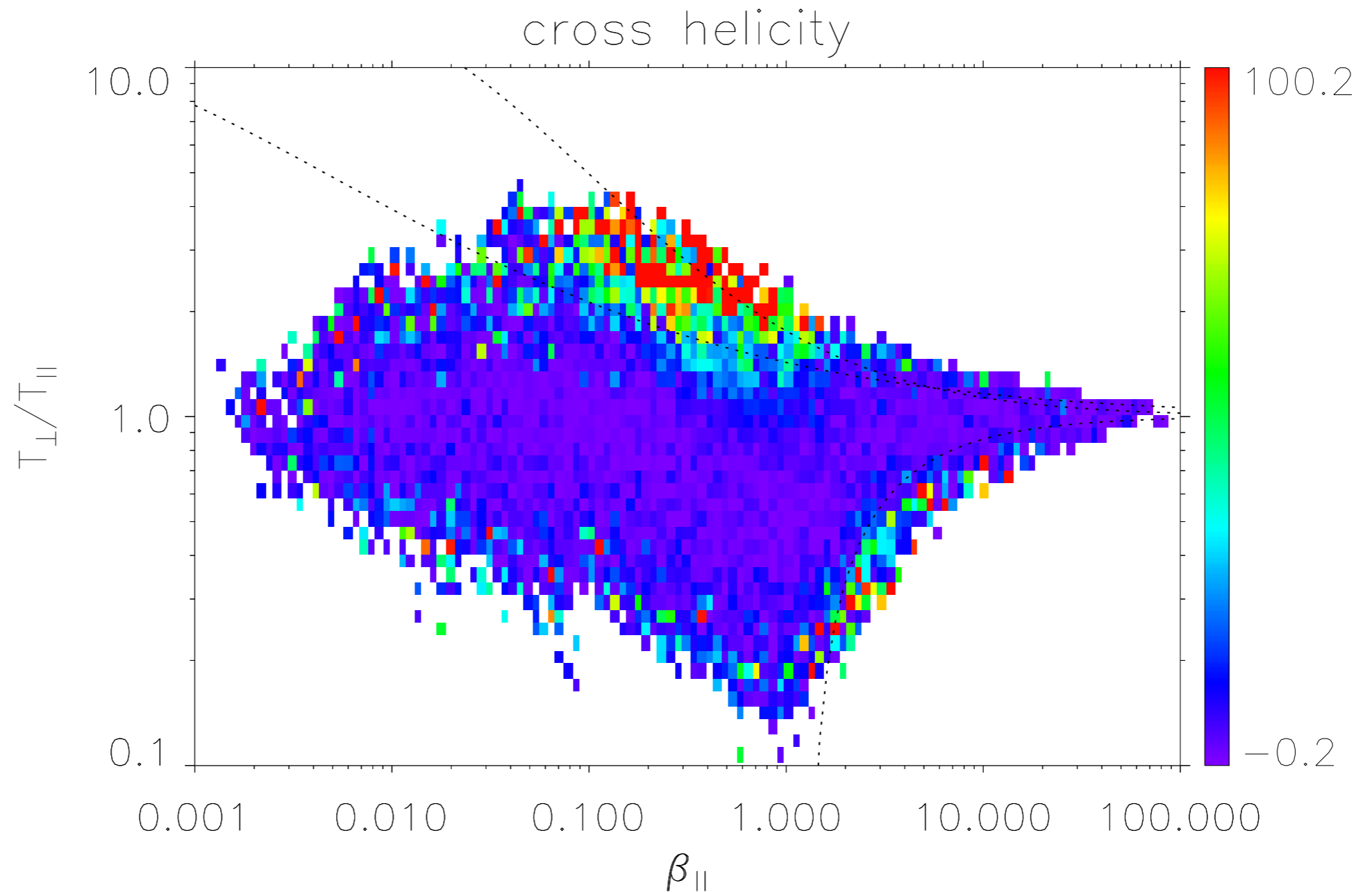
- black = isotropic, red = perp anisotropy, blue = parallel anisotropy
- white noise removed
- power at this intensity and bandwidth appears in the 'dissipation' (KAW) range
- any meaningful study of turbulent (wave-wave) dissipation must address the locally generated fluctuations



# Proton anisotropy instabilities - $\delta v$ data

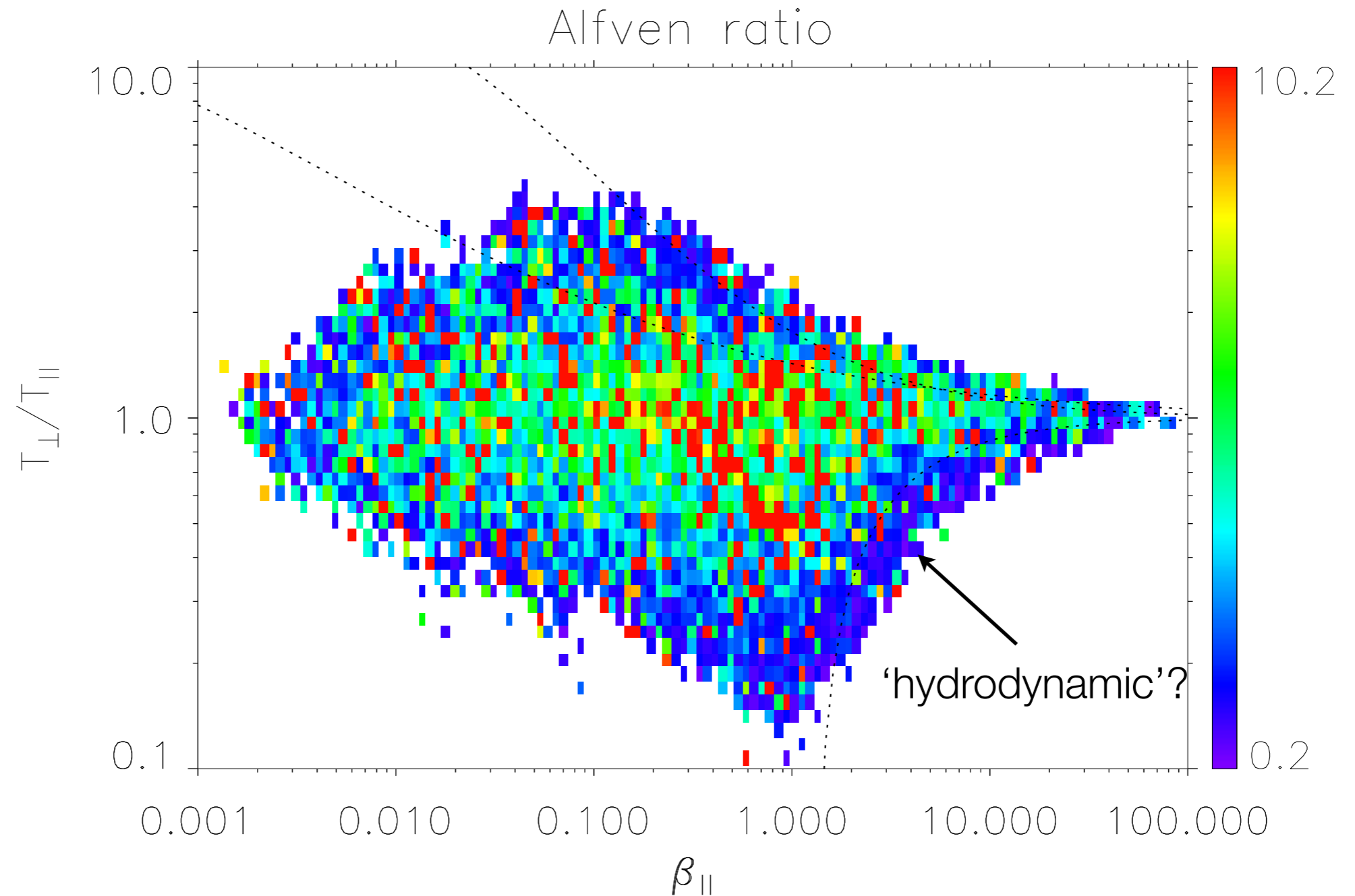


# Proton anisotropy instabilities - new things



$$\langle \delta v \cdot \delta b \rangle \quad (\Delta t = 3 \text{ sec}, T = 15 \text{ sec})$$

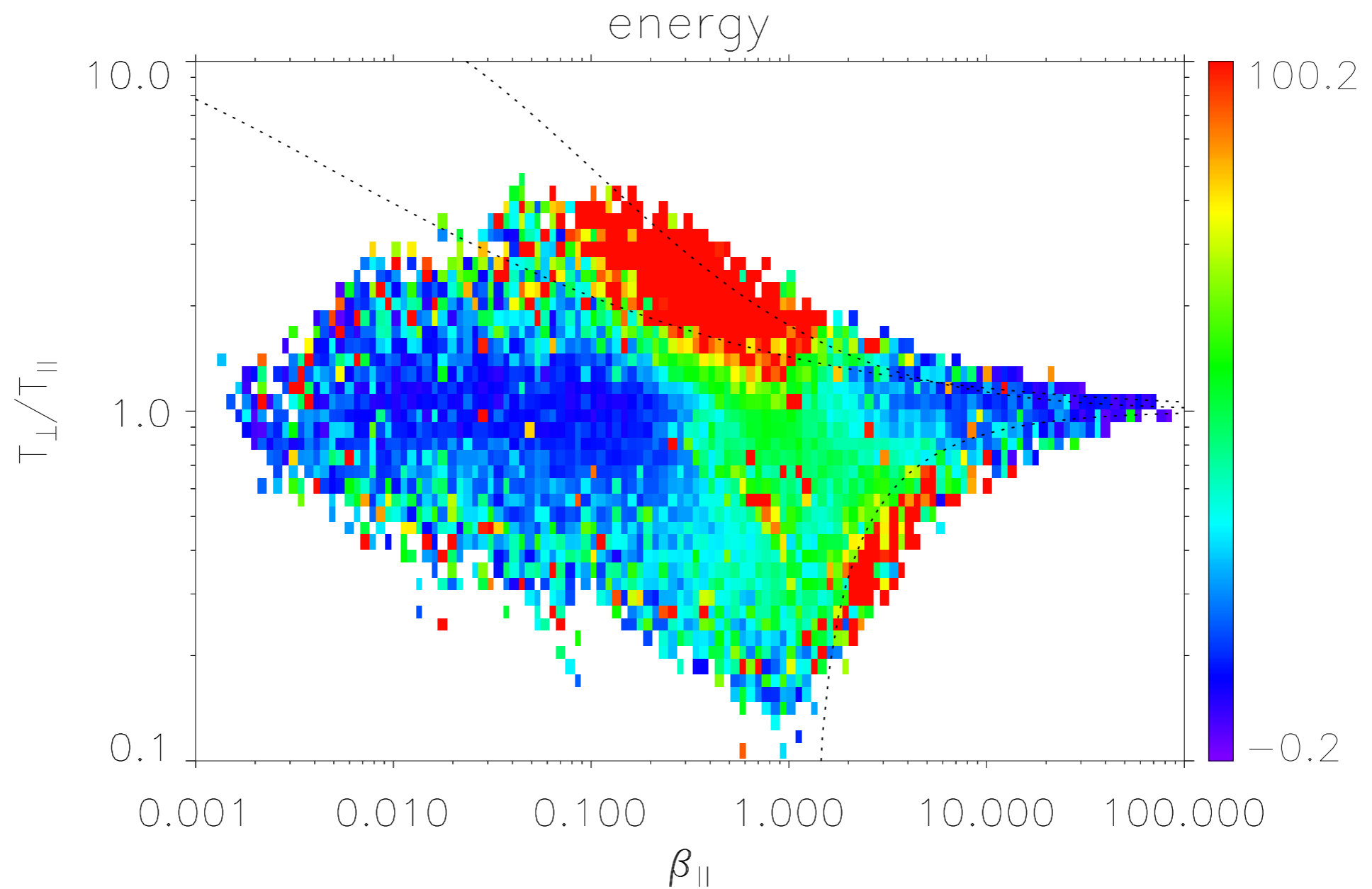
# Proton anisotropy instabilities - new things



$$\langle (\delta v)^2 / (\delta b)^2 \rangle \quad (\Delta t = 3 \text{ sec}, T = 15 \text{ sec})$$

# Proton anisotropy instabilities - new things

---



$$\langle (\delta v)^2 + (\delta b)^2 \rangle \quad (\Delta t = 3 \text{ sec}, T = 15 \text{ sec})$$

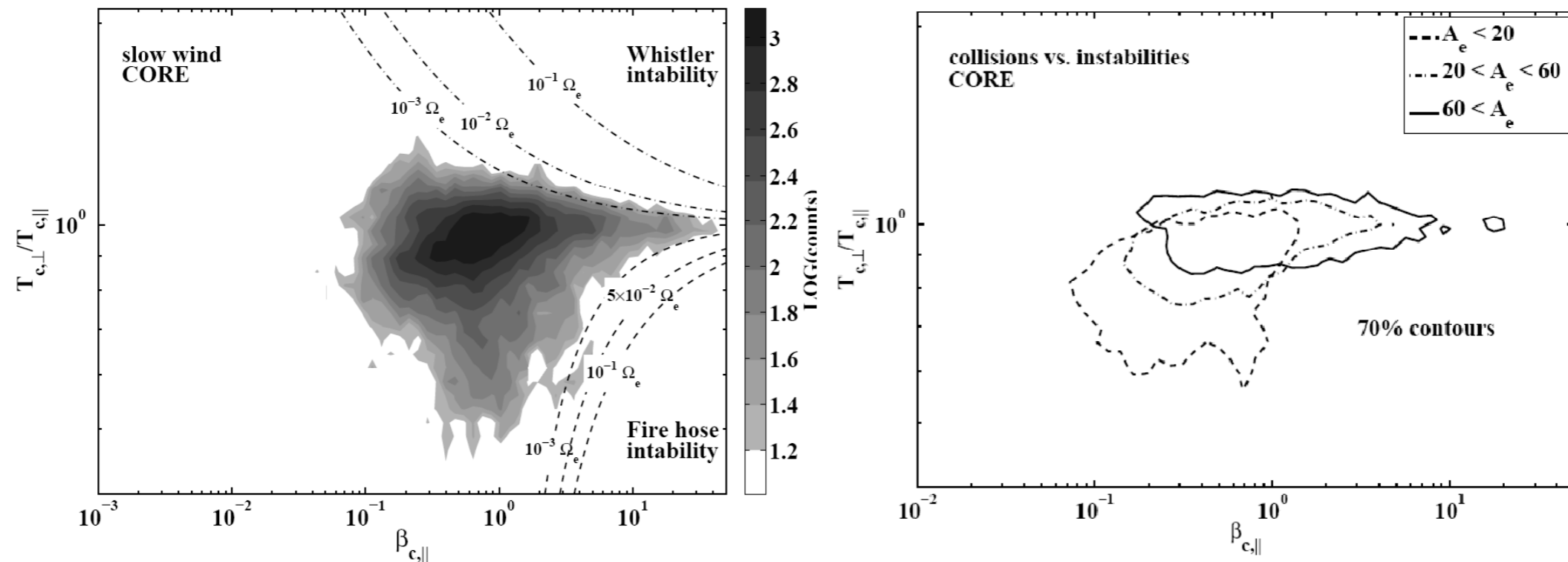
# anisotropic viscous stress

---

$$W_{r\phi} = - \left( 1 - \frac{p_{\parallel} - p_{\perp}}{B^2} \right) \frac{B_r B_{\phi}}{4\pi} + \rho v_r \delta v_{\phi}$$

- can be comparable to the Maxwell stress in astrophysical plasmas
- results in ion and electron heating
- constrained by  $\mu$  invariance and instabilities

# Evidences for both collisions and instabilities shaping the eVDFs



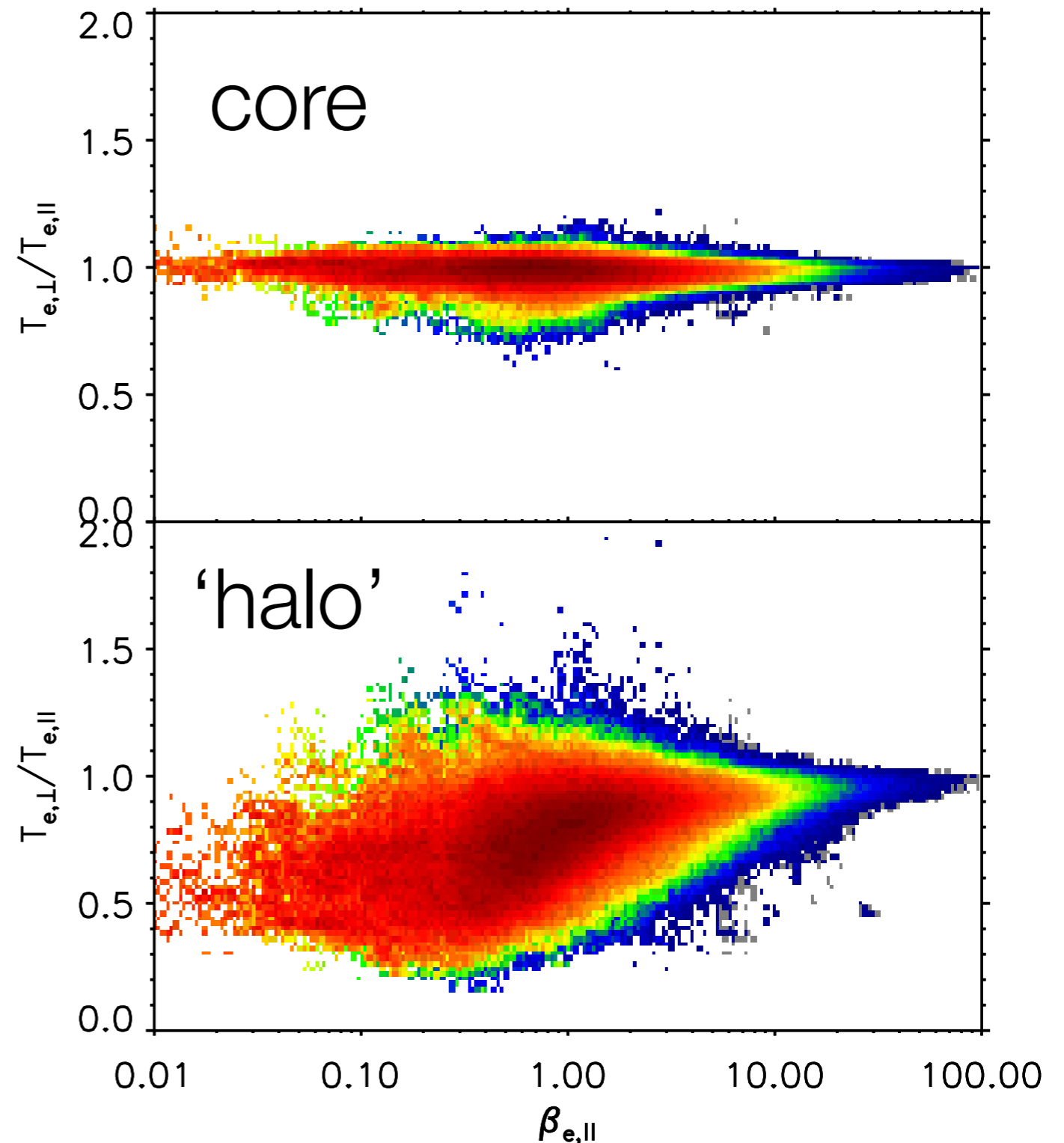
$$A_e = v_{ee} \frac{R}{V} : \text{collisional age}$$

Stverak et al., JGR, 2008

Similar for protons : Kasper et al., Hellinger et al.

# electron anisotropies

- Wind/3DP electron distributions at same time intervals as before  
~ 1 million independent measurements
- corrected for spacecraft potential using SWE moments
- integrated into two populations:
  - core: 0 - 80 eV
  - halo: 80 - 1000 eV (anisotropy only)
- core is very isotropic - collisions
- halo is ordered by electron  $\beta$

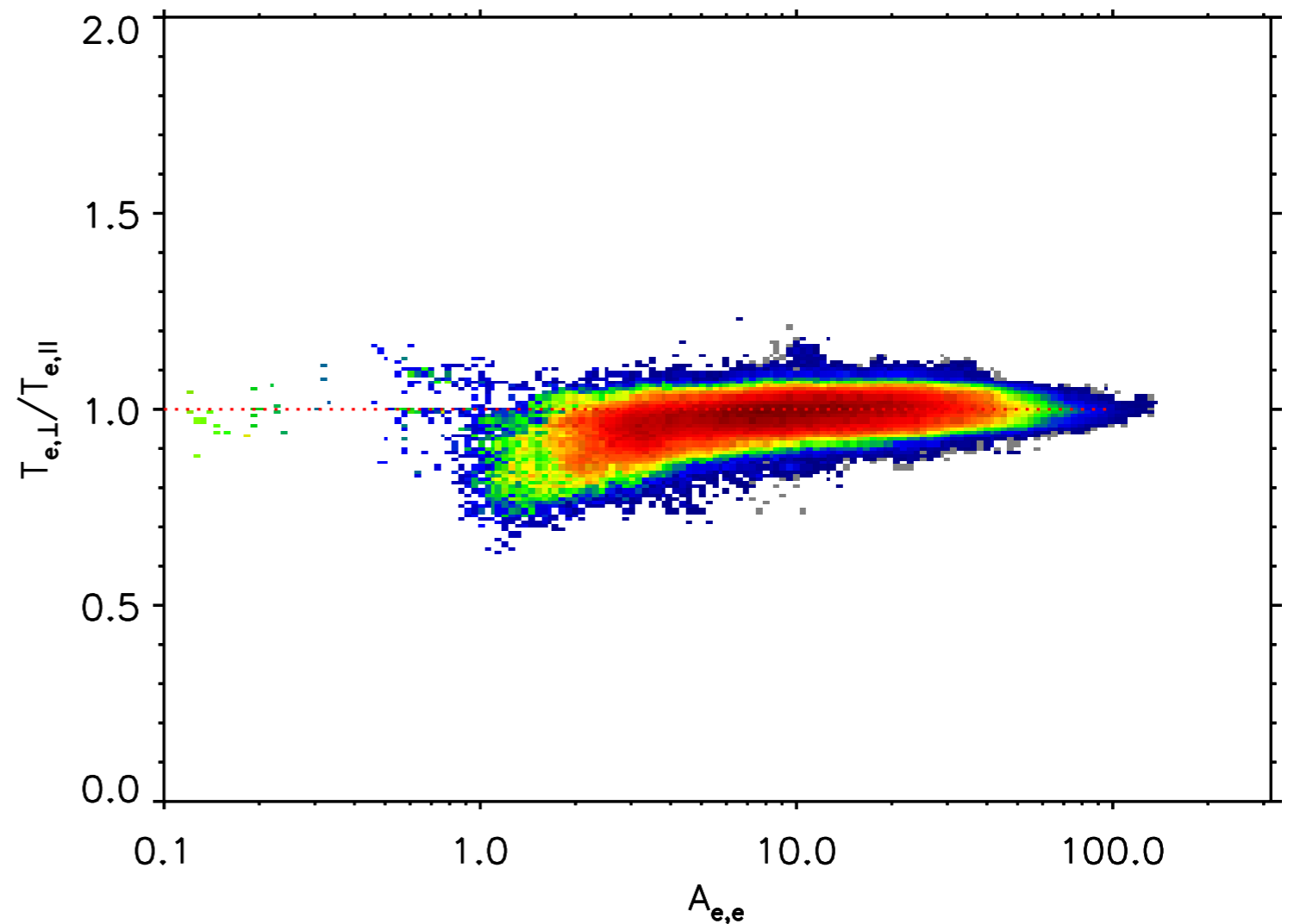




# core anisotropy vs collisional age

---

- a 'collisional age' can be estimated from collision frequency and transit time (viz. Salem et al)
- core electrons appear to be well-ordered by collisions (here, at 1 AU)
- some anisotropy consistent with conservation of magnetic moment



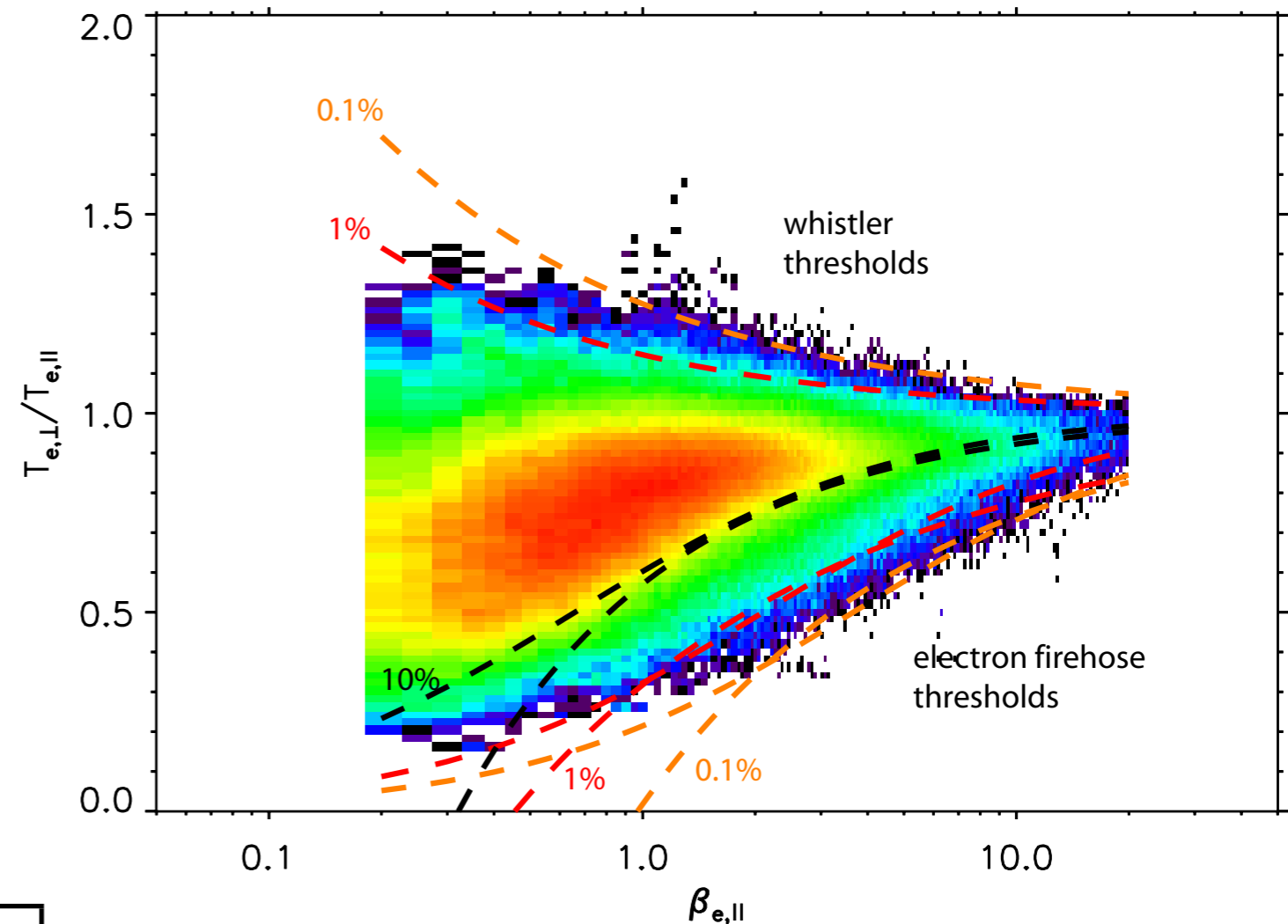
# Halo anisotropies are constrained by instabilities

- halo is constrained by a whistler instability for  $T_{\perp}/T_{\parallel} > 1$
- halo is constrained by the electron firehose instability for  $T_{\perp}/T_{\parallel} < 1$

$$T_{\perp}/T_{\parallel} < 1 + S/\beta_{e,\parallel}^{\alpha}$$

whistler      e- firehose

count level	S	$\alpha$	S	$\alpha$
0.1%	0.275	0.577	-0.982	0.579
1%	0.147	0.647	-0.682	0.485
10%	-	-	-0.429	0.744



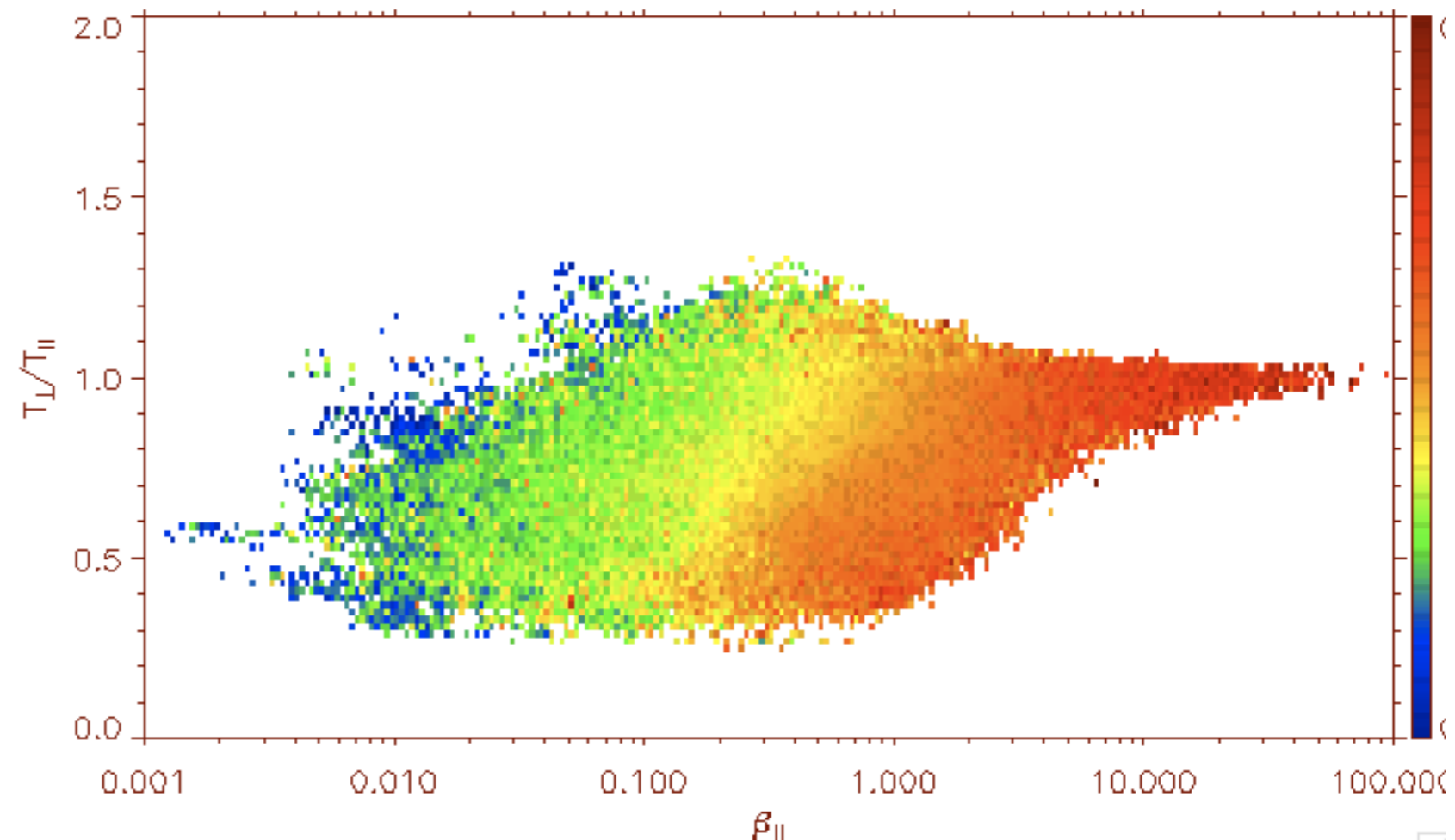
# Halo anisotropies are constrained by instabilities

---

- halo is constrained by a whistler instability for  $T_{\perp}/T_{\parallel} > 1$

Wind SCM data - ~20 Hz

- halo is constrained by the electron firehose instability for  $T_{\perp}/T_{\parallel} < 1$



# Conclusions

---

- Solar wind requires heating, both at the source and extended
- Extended, distributed heating implies turbulent dissipation
- Resistively-coupled electric field measurements provide critical diagnostics
- Local instabilities generate power in precisely the same spectral range as turbulent dissipation occurs
- Excellent opportunities for these measurements on the next generation of solar wind missions.

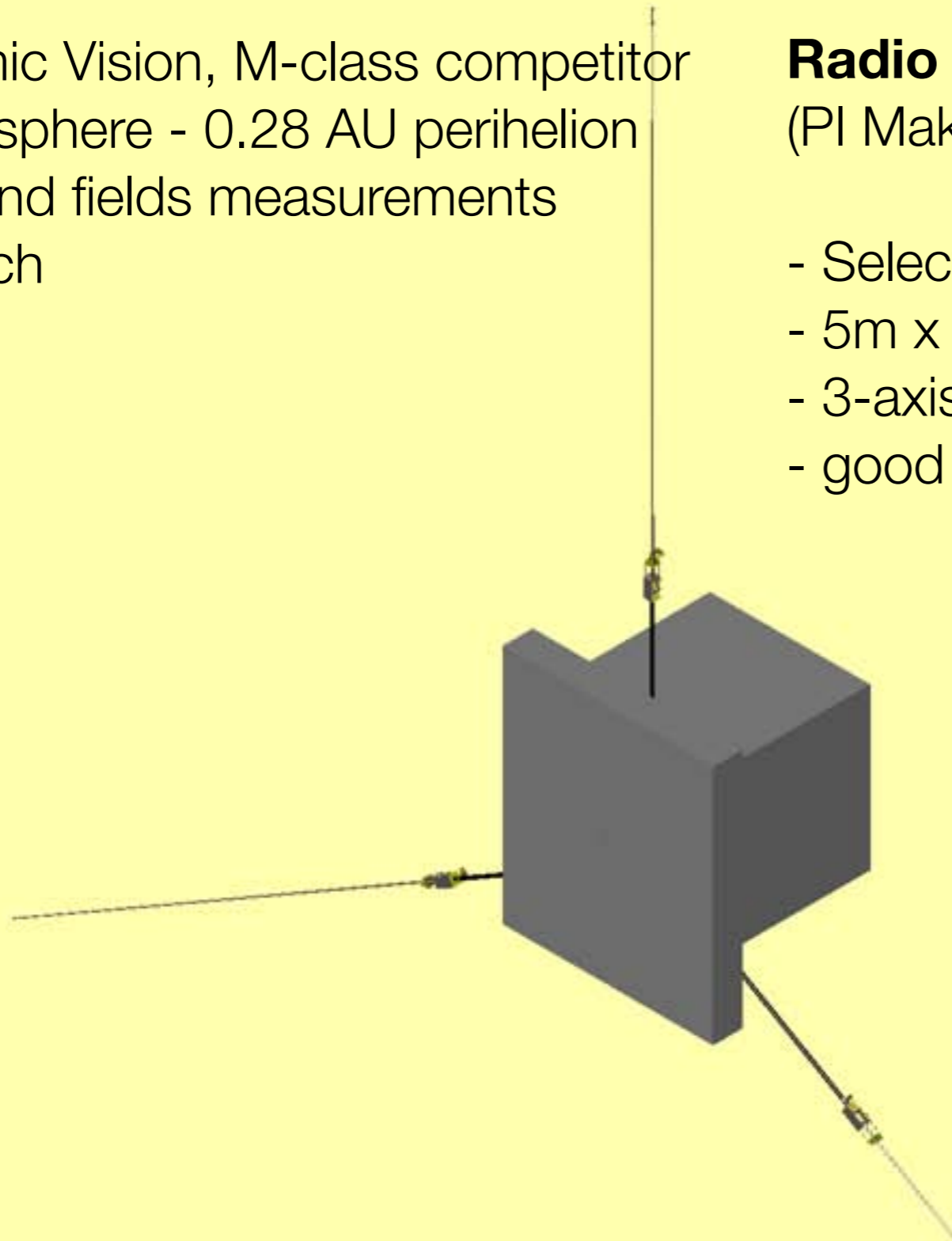
# Solar Orbiter RPW Instrument

---

- ESA Cosmic Vision, M-class competitor
- Inner heliosphere - 0.28 AU perihelion
- Particles and fields measurements
- 2017 launch

## **Radio and Plasma Waves = RPW** (PI Maksimovic)

- Selected with 3 antenna booms
- 5m x 1.5 cm sensor on a 1m boom
- 3-axis stable spacecraft
- good and stable Sun symmetry



# Solar Probe Plus

- NASA LWS mission
- Inner heliosphere - 9.5  $R_s$  perihelion
- Particles and fields measurements
- 2018 launch
- nasty plasma wake

